nature genetics

Letter

https://doi.org/10.1038/s41588-026-02713-9

APOE-stratified genome-wide association analyses provide insights into the genetic etiology of Alzheimers's disease

Received: 6 May 2025

Accepted: 14 July 2026

Published online: 14 September 2026

Check for updates

A list of authors and their affiliations appears at the end of the paper

Among the more than 90 identified genetic risk loci for late-onset Alzheimer's disease (AD) and related dementias, the apolipoprotein E (*APOE*) gene ε2/ε3/ε4 polymorphisms remain the longstanding benchmark for genetic disease risk with a consistently large effect across studies[1–10]. Despite this massive signal, the exact mechanisms by which ε4 increases and ε2 decreases dementia risk remain poorly understood. Notably, recent trials of anti-amyloid therapies suggest less efficacy and higher risks of severe side effects in ε4 carriers[11–13], hampering the treatment of those with the highest unmet need. To improve our understanding of the genetic architecture of AD in the context of its main genetic driver, we performed genome-wide association studies (GWASs) stratified by ε4 and ε2 carrier status. *HP1BP3*, *SLC50A1*, *PTPRC*, *NPAS3*, *DDHD1*, *CHST9*, *SMYD2*, *PRAMEF1* and *GFRA1* emerged as new genomic signals for AD risk, appearing only when stratified by *APOE* carrier status. *DDHD1* appeared especially promising, showing protective effects in ε4 carriers, being identified as an expression quantitative trait locus and being involved in rare neuronal diseases. Such *APOE*-stratified insights may help understand and overcome side effects, inform clinical trial enrollment strategies, and create the scientific basis for targeted, mechanism-driven therapies in neurodegenerative diseases.

We performed a large genome-wide association study (GWAS) meta-analysis stratified by apolipoprotein E (*APOE*) ε2/ε3/ε4 status, bringing together European, Asian, Asian American (AAC), African American (AFR) and admixed American (AMR) ancestry cohorts based on the clinically diagnosed Alzheimer's disease (AD). An overview of the included consortia and cohorts, as well as the analysis strategy, is shown in Extended Data Fig. 1. Individuals were grouped into ε22 + ε32, ε33 and ε44 + ε43 strata to maximize statistical power, and individuals with the ε42 genotype were excluded (Supplementary Tables 1 and 2). In the ε22 + ε32 stratum, the meta-analysis was based on 2,606 AD cases, 70,388 controls and 10,336,311 variants (Supplementary Table 3 and Supplementary Fig. 1). In the ε33 stratum, the meta-analysis was based on 24,033 AD cases, 363,161 controls and 17,127,662 variants (Supplementary Table 4 and Supplementary Fig. 1). In the ε44 + ε43 stratum, the meta-analysis was based on 29,122 AD cases, 164,206 controls and 14,672,059 variants (Supplementary Table 5 and Supplementary Fig. 1, and for strata ε44, see Supplementary Table 6 and Supplementary Fig. 1).

For the ε22 + ε32 stratum, no signal reached a genome-wide significance level of $<2.5 \times 10^{-8}$ (Supplementary Fig. 2). In total, 25 loci reached a genome-wide significance level in stratum ε33 or ε44 + ε33 only or in both (Fig. 1, Table 1 and Supplementary Figs. 4–24). The nine loci found in both strata are known genetic risk loci for AD (*CR1*, *BIN1*, *HLA*, *TREM2*, *CLU*, *MS4A64*, *PICALM*, *APH1B*, *ABCA7*). Nine loci were exclusively observed in the ε44 + ε43 stratum, including six known AD loci (*PILRA*, *SORL1*, *ADAM10*, *ACE*, *LILRA5*, *CASS4*) and three new loci

e-mail: jesper.qvist.thomassen@regionh.dk; mike@datatecnica.com; ruth.frikke-schmidt@regionh.dk

https://doi.org/10.1038/s41588-026-02713-9

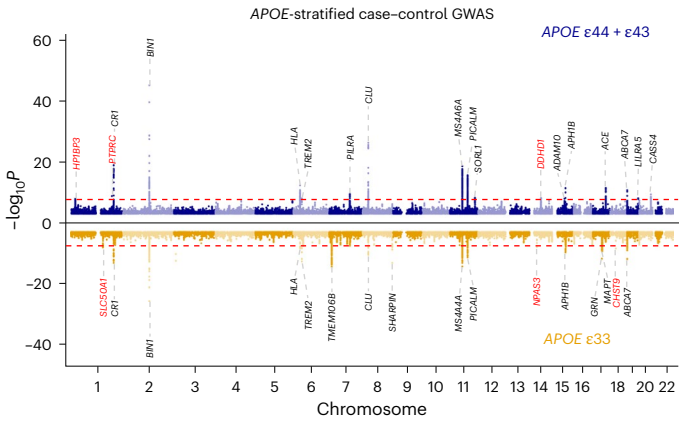


Fig. 1 | Miami plot of the *APOE* ε33 and ε44 + ε43 strata. Top: the Manhattan plot for the *APOE* ε44 + ε43 strata is shown in blue. Bottom: the Manhattan plot for the *APOE* ε33 strata is shown in orange in the lower part. Genome-wide significant loci are annotated with the nearest genes (known loci in black and new in red). Two-sided raw *P* values were derived from a fixed-effect meta-analysis. The red dashed lines show the genome-wide significant level for two GWASs ($P = 2.5 \times 10^{-8}$).

(*HP1BP3*, *PTPRC*, *DDHD1*). Notably, *DDHD1* is close to the *FERMT2* locus, which is recognized as a genetic risk factor for AD. However, using conditional testing, we found that the *DDHD1* signal is independent of *FERMT2* (Fig. 1 and Supplementary Table 7). Finally, among seven loci only reaching genome-wide significance level in the ε33 stratum, four are known AD risk loci (*TMEM106B*, *SHARPIN*, *GRN*, *MAPT*) and three are new (*SCL50A1*, *NPAS3*, *CHST9*).

Of note, we also performed a meta-analysis restricted to the ε44 carriers. Only one well-established locus (*BIN1*) was observed in the ε44 stratum, including 5,814 AD cases, 14,415 controls and 9,723,486 variants (Supplementary Table 6 and Supplementary Fig. 3). Forest plots across cohorts and strata are shown in Supplementary Figs. 25–53. In addition, we applied clumping procedures and conditional testing to define potential independent signals within each locus detected in the ε33 and ε44 + ε43 strata. This approach detected four loci presenting two independent signals (*HLA-DRA*, *TREM2*, *CLU*, *APH1B*; Supplementary Table 7); details are specified in the legend of Table 1.

The present meta-analyses do not allow us to fully determine whether there is a significant difference between the signals observed in the ε33 and ε44 + ε43 strata due to sample and statistical power variations. To formally test for nucleotide polymorphism (SNP) × *APOE* interactions, we used two complementary approaches. First, we performed interaction tests based on stratified effect comparisons using additive and dominant models with summary statistics from the different *APOE* strata, testing only variants that were significant in one or both strata. Second, we conducted a genome-wide SNP × *APOE* ε4 carrier interaction GWAS using a formal interaction term in a unified model.

In the stratified effect comparison testing dominant *APOE* ε4 effects (meta-analysis of differences between ε33 and ε44 + ε43 in each cohort), we found the following seven significant stratified effect differences: three signals where the effect sizes were attenuated with the presence of an ε4 allele (*SLC50A1*, *TMEM106B*, *NPAS3*; Table 2 and Fig. 2), and four signals where the effect sizes were augmented with the presence of an ε4 allele (*BIN1*, *HLA-DRA*-1, *CLU*, *DDHD1*; Table 2 and Fig. 3). Forest plots of the effect differences across cohorts are shown in Supplementary Figs. 54 and 55. In the additive mixed-effect model, we additionally identified *SHARPIN* as interacting with *APOE* ε4, where the effect size was attenuated with an increasing number of ε4 alleles (Table 2 and Fig. 2). Stratified effect-difference sensitivity analyses are shown in Supplementary Table 8.

In the genome-wide SNP × *APOE* ε4 carrier interaction GWAS, two new loci (*SMYD2* and *ANK3*) reached genome-wide significance in the SNP term (comparable to *APOE* ε33 strata; Supplementary Fig. 56 and Supplementary Table 9). The *APOE* ε4 carrier term was highly significant ($P < 1 \times 10^{-300}$) and SNP independent. In the interaction term (SNP × *APOE* ε4 carrier), only the *APOE* locus was significant. However, the *DDHD1* locus reached an interaction *P* value of 1.62×10^{-6}. The loci with an interaction *P* value below 1×10^{-5} are shown in Supplementary Table 10, and the results from the interaction GWAS for the 29 regions of interest are shown in Supplementary Table 11.

We evaluated the 29 regions of interest in additional cohorts of East Asian (EAS) ancestry, representing Japanese (JADNI, CL, NP; EAS-JPN), Chinese (HKS; EAS-CHN) and Korean (GARD; EAS-KOR) populations, as well as in AAC (ADSP-AAC), AFR (ADSP-AFR) and AMR (ADSP-AMR) multi-ancestry populations (Supplementary Table 12). Despite several limitations (that is, difference in linkage structure across cohorts of different ancestries, limitation in statistical power and lead variants being different from the causal variants), similar signals could be observed for several variants (Supplementary Figs. 57–83). The meta-analyzed results for *HLA-DRA*-1 and *DDHD1* were similar in the East Asian ancestry cohorts compared with the European ancestry cohorts (Fig. 4).

For lead variant rs10131116 in *DDHD1*, a significant expression quantitative trait locus (eQTL) associated with decreased *DDHD1* expression was observed in the ROSMAP dorsolateral prefrontal cortex ($\beta = -0.098$; eQTL, $P = 1.67 \times 10^{-5}$, $n = 560$)[6] and in the GTEx (v10) brain putamen (basal ganglia; https://www.gtexportal.org/home/snp/rs10131116; $\beta = -0.23$; eQTL, $P = 3.6 \times 10^{-5}$, $n = 253$)[14]. We tested whether rs10131116 was associated with lower *DDHD1* expression according to *APOE* strata and observed nominal *P* values of 9×10^{-4} for ε33 and 7×10^{-3} for ε44 + ε43 (Supplementary Table 13 and Supplementary Fig. 84). Furthermore, a gene-based analysis confirmed several of the significant loci from the main stratified GWAS analysis (Extended Data Fig. 2). Also, in the ε44 + ε43 stratum, the known AD genes *EPHA1*, *TCPN1* and *BLNK* reached significance, and, in the ε33 stratum, the known AD genes *SLC24A4*, *INPP5D* and *SH2B2* (new but close to the known locus *SPDYE3*/*PILRA*/*TMEM225B*) reached significance. *ACE* and *SNX1* were significant in both the ε44 + ε43 and ε33 strata, whereas *PRAMEF1* was significant in the ε44 stratum and *GFRA1* in the ε22 stratum (Extended Data Fig. 2 and Supplementary Tables 14–17). Next, we performed a pathway enrichment analysis on the *APOE*-stratified GWAS results from the eight European ancestry studies (Supplementary Tables 18 and 19). After correction for multiple testing in each stratum ($q < 0.05$), 12 and 33 pathways reached statistical significance for the *APOE* ε33 and ε44 + ε43 strata, respectively. Overall, pathways related to the complement and immune systems were over-represented in the *APOE* ε44 + ε44 stratum compared to the ε33 stratum, whereas amyloid and neurofibrillary tangle biology was highlighted in both strata. No pathway analysis reached statistical significance for the ε22 + ε32 nor for the ε43 stratum. Finally, we performed summary-data-based Mendelian randomization (SMR) to test for potential effects of expression on AD that are shared by a causal variant for both *APOE* ε4 carriers (ε44 + ε43) and noncarriers (ε33). Four genes passed our significance threshold and HEIDI filtering—*STAG3* (*PILRA* locus) in the ε44 + ε43 stratum (cortex) and *LRRC37A*, *ARL17B* and *LRRC37A2* (*MAPT* locus) in the ε33 stratum (multiple brain regions; Supplementary Table 20).

By conducting a comprehensive series of *APOE*-stratified GWAS analyses, we identified a number of biologically plausible genomic signals that modify the effect of the *APOE* ε4 allele. As these findings suggest differential biological pathways dependent on the *APOE* strata, they may inform how we use genetics in designing randomized clinical trials of future AD medicines.

HP1BP3, *SLC50A1*, *PTPRC*, *NPAS3*, *DDHD1* and *CHST9* from the stratified variant-based GWAS analysis, *SMYD2* from the interaction GWAS and *PRAMEF1* and *GFRA1* from the gene-based analysis are new genomic signals for AD risk, only appearing when stratified by *APOE* carrier status, and supported by significant stratified effect comparison tests for

Table 1 | Genome-wide significant association signals

topmed_id[a]	Chromosome	Position[b]	Ref	Eff	rsid[c]	Locus[d]	Gene[d]	*APOE* ε33				*APOE* ε44+ε43			
								EAF	OR (95% CI)[e]	*P* value[f]	I^{2g}	EAF	OR (95% CI)[e]	*P* value[f]	I^{2g}
Chr1: 20,745,474:C:T	1	20745474	C	T	rs2274119	*HP1BP3*	*HP1BP3*	0.074	1.03 (0.99–1.08)	0.165	11.1	0.072	**1.15 (1.10–1.21)**	**1.33×10^{-8}**	0
Chr1: 155,135,691:G:A	1	155135691	G	A	rs12726330	*SLC50A1*	*SLC50A1*	0.037	**1.22 (1.14–1.31)**	**8.17×10^{-9}**	0	0.038	1.00 (0.93–1.07)	0.937	10.3
Chr1: 198,710,886:G:A	1	198710886	G	A	rs12733073	*PTPRC*	*PTPRC*	0.010	1.20 (1.07–1.35)	1.81×10^{-3}	0	0.010	**1.46 (1.29–1.65)**	**1.63×10^{-9}**	38.1
Chr1: 207,577,223:T:C	1	207577223	T	C	rs679515	*CR1*	*CR1*	0.81	**0.91 (0.88–0.93)**	**8.30×10^{-12}**	33.8	0.70	**0.87 (0.84–0.90)**	**1.44×10^{-19}**	55.2
Chr2: 127,135,234:C:T	2	127135234	C	T	rs6733839	*BIN1*	*BIN1*	0.38	**1.14 (1.11–1.16)**	**2.30×10^{-26}**	64.6	0.38	**1.20 (1.17–1.23)**	**9.88×10^{-46}**	58.3
Chr6: 32,411,770:C:T	6	32411770	C	T	rs17208902	*HLA-DRA*[h]	*HLA-DRA*-1	0.25	1.03 (1.00–1.06)	0.0409	0	0.26	**1.11 (1.08–1.14)**	**4.82×10^{-13}**	10.2
Chr6: 32,464,090:G:T	6	32464090	G	T	rs9268888	*HLA-DRA*[h]	*HLA-DRA*-2	0.54	**0.93 (0.91–0.96)**	**4.57×10^{-9}**	0	0.54	0.94 (0.92–0.96)	7.60×10^{-7}	54.3
Chr6: 41,161,469:C:T	6	41161469	C	T	rs143332484	*TREM2*[h]	*TREM2*-1	0.011	1.29 (1.16–1.44)	3.27×10^{-6}	15.9	0.011	**1.43 (1.27–1.62)**	**9.11×10^{-9}**	7.4
Chr6: 41,161,514:C:T	6	41161514	C	T	rs75932628	*TREM2*[h]	*TREM2*-2	0.0029	**2.78 (2.12–3.66)**	**2.37×10^{-13}**	0	0.0032	**2.18 (1.66–2.85)**	**1.30×10^{-8}**	42.2
Chr7: 12,242,825:T:C	7	12242825	T	C	rs7805419	*TMEM106B*	*TMEM106B*	0.38	**0.91 (0.89–0.93)**	**4.14×10^{-15}**	22.7	0.37	0.97 (0.94–0.99)	8.98×10^{-3}	46.4
Chr7: 100,386,466:T:C	7	100386466	T	C	rs2906657	*PILRA*	*PILRA*	0.30	0.94 (0.91–0.96)	4.71×10^{-7}	0	0.30	**0.92 (0.89–0.94)**	**3.39×10^{-10}**	44.1
Chr8: 27,362.470:C:T	8	27362470	C	T	rs73223431	*CLU*[i]	*PTK2B*	0.37	1.06 (1.04–1.09)	7.41×10^{-7}	43.8	0.37	**1.10 (1.07–1.13)**	**4.30×10^{-14}**	0
Chr8: 27,610,986:C:A	8	27610986	C	A	rs867230	*CLU*[i]	*CLU*	0.57	**1.08 (1.06–1.11)**	**5.32×10^{-11}**	21.9	0.57	**1.15 (1.12–1.18)**	**6.21×10^{-27}**	0
Chr8: 144,103,704:G:A	8	144103704	G	A	rs34173062	*SHARPIN*	*SHARPIN*	0.075	**1.19 (1.14–1.25)**	**7.77×10^{-14}**	4.7	0.070	1.08 (1.02–1.14)	4.62×10^{-3}	20.2
Chr11: 60,173,126:T:A	11	60173126	T	A	rs7232	*MS4A6A*	*MS4A6A*	0.34	**0.91 (0.89–0.93)**	**7.67×10^{-14}**	0	0.33	**0.89 (0.86–0.91)**	**2.62×10^{-19}**	44.9
Chr11: 86,113,817:A:G	11	86113817	A	G	rs659023	*PICALM*[j]	*PICALM*	0.60	1.07 (1.04–1.10)	4.03×10^{-8}	43.8	0.58	**1.11 (1.09–1.14)**	**2.27×10^{-16}**	11.6
Chr11: 86,141,937:G:A	11	86141937	G	A	rs10792831	*PICALM*[j]	*PICALM*	0.54	1.09 (1.06–1.11)	**4.42×10^{-12}**	41.2	0.56	1.09 (1.06–1.11)	**2.75×10^{-11}**	0
Chr11: 121,564,878:T:C	11	121564878	T	C	rs11218343	*SORL1*	*SORL1*	0.034	0.89 (0.83–0.95)	2.47×10^{-4}	49.6	0.032	**0.81 (0.75–0.87)**	**5.60×10^{-9}**	0
Chr14: 33,428,905:G:C	14	33428905	G	C	rs187023552	*NPAS3*	*NPAS3*	0.016	**1.42 (1.26–1.61)**	**1.04×10^{-8}**	0	0.015	0.98 (0.86–1.11)	0.722	82.6
Chr14: 53,394,351:T:C	14	53394351	T	C	rs10131116	*FERMT2*	*DDHD1*	0.37	1.02 (1.00–1.05)	0.0416	43.0	0.37	**0.93 (0.90–0.95)**	**6.61×10^{-9}**	0
Chr15: 58,790,588:T:G	15	58790588	T	G	rs347116	*ADAM10*	*ADAM10*	0.39	0.96 (0.94–0.98)	9.04×10^{-4}	0	0.40	**0.93 (0.90–0.95)**	**1.11×10^{-8}**	0
Chr15: 63,279,621:C:T	15	63279621	C	T	rs75763893	*APH1B*[i]	*APH1B*	0.13	**1.12 (1.08–1.15)**	**2.22×10^{-10}**	40.5	0.13	**1.14 (1.10–1.18)**	**3.87×10^{-12}**	32.6
Chr15: 63,407,216:C:T	15	63407216	C	T	rs181364771	*APH1B*[i]	*LINC02568*	0.028	**1.27 (1.18–1.37)**	**1.34×10^{-9}**	30	0.029	1.18 (1.09–1.28)	7.69×10^{-5}	21.8
Chr17: 44,352,876:C:T	17	44352876	C	T	rs5848	*GRN*	*GRN*	0.32	**1.09 (1.07–1.12)**	**1.74×10^{-12}**	0	0.32	1.05 (1.03–1.08)	1.24×10^{-4}	0
Chr17: 46,111,701:A:G	17	46111701	A	G	rs7225002	*MAPT*	*MAPT* H2	0.38	**0.93 (0.91–0.95)**	**4.88×10^{-10}**	36.4	0.39	0.97 (0.95–1.00)	0.0320	31.1
Chr17: 63,470,201:G:A	17	63470201	G	A	rs8077276	*ACE*	*ACE*	0.58	1.05 (1.03–1.08)	1.10×10^{-5}	0	0.58	**1.09 (1.07–1.12)**	**3.45×10^{-12}**	14.7
Chr18: 27,352,028:C:A	18	27352028	C	A	rs544488330	*CHST9*	*CHST9*	0.0025	**2.21 (1.70–2.88)**	**3.69×10^{-9}**	70.1	0.0019	1.32 (0.85–2.06)	0.220	4.8
Chr19: 1,050,875:A:G	19	1050875	A	G	rs12151021	*ABCA7*	*ABCA7*	0.64	**0.91 (0.89–0.94)**	**1.47×10^{-12}**	70.7	0.63	**0.91 (0.89–0.94)**	**6.75×10^{-11}**	16.6
Chr19: 54,304,006:C:T	19	54304006	C	T	rs1761453	*LILRA5*	*LILRA5*	0.45	0.97 (0.95–0.99)	9.65×10^{-3}	48.8	0.45	**0.93 (0.91–0.95)**	**8.53×10^{-9}**	0
Chr20: 56,449,045:G:A	20	56449045	G	A	rs113221226	*CASS4*	*CASS4*	0.069	0.91 (0.87–0.96)	1.88×10^{-4}	37.8	0.063	**0.84 (0.79–0.89)**	**4.34×10^{-10}**	0

[a] TOPMed r^2 identifier. [b] GRCh38 assembly. [c] Reference SNP (rs) numbers, according to dbSNP build 156. [d] Nearest protein-coding or long intergenic nonprotein-coding RNA according to Ensembl release 111. [e]OR and 95% CI calculated with respect to the effect allele. [f]Two-sided raw *P* values derived from a fixed-effect meta-analysis. $P<2.5\times10^{-8}$ is considered genome-wide significant due to multiple GWAS strata tested. Significant *P* values and corresponding ORs are in bold. [g] Heterogeneity I^2 statistics. [h]In the *HLA-DRA* and *TREM2* loci, different independent variants reached genome-wide significance level in the two strata. [i]In the *CLU* and *APH1B* loci, a second independent variant reached genome-wide significance in one of the strata. [j] In the *PICALM* locus, two different variants in the two strata reached genome-wide significance and had the lowest *P* value in the locus. However, the two variants were in LD ($r^2>0.4$). CI, confidence intervals; EAF, effect allele frequency; OR, odds ratio.

https://doi.org/10.1038/s41588-026-02713-9

Table 2 | Interaction testing results

topmed_id[a]	rsid[b]	Locus	Gene[c]	Dominant interaction—effect difference					Additive interaction—per ε4 allele				
				Δβ[d]	s.e.	*P* value[e]	I^{2f}	Het *P* value[g]	β[h]	s.e.	*P* value	I^{2f}	Het *P* value[g]
Chr1: 20,745,474:C:T	rs2274119	*HP1BP3*	*HP1BP3*	0.092	0.034	7.2×10^{-3}	0	0.97	0.062	0.027	0.025	23	0.18
Chr1: 155,135,691:G:A	**rs12726330**	***SLC50A1***	***SLC50A1***	**−0.19**	**0.051**	**1.6×10^{-4}**	0	0.80	**−0.13**	**0.040**	**1×10^{-3}**	35	0.098
Chr1: 198,710,886:G:A	rs12733073	*PTPRC*	*PTPRC*	0.20	0.089	0.026	19	0.28	0.13	0.073	0.086	0.58	0.44
Chr1: 207,577,223:T:C	rs679515	*CR1*	*CR1*	−0.045	0.022	0.038	46	0.072	−0.021	0.017	0.226	52	4.1×10^{-3}
Chr2: 127,135,234:C:T	**rs6733839**	***BIN1***	***BIN1***	**0.064**	**0.018**	**3.7×10^{-4}**	0	0.73	0.045	0.014	1.5×10^{-3}	58	**6.5×10^{-4}**
Chr6: 32,411,770:C:T	**rs17208902**	***HLA-DRA***	***HLA-DRA*-1**	**0.078**	**0.020**	**1.1×10^{-4}**	0	0.59	**0.057**	**0.016**	**3.6×10^{-4}**	0	0.60
Chr6: 32,464,090:G:T	rs9268888	*HLA-DRA*	*HLA-DRA*-2	0.0089	0.018	0.61	0	0.55	−0.0027	0.014	0.85	24	0.16
Chr6: 41,161,469:C:T	rs143332484	*TREM2*	*TREM2*-1	0.098	0.085	0.25	0	0.74	0.087	0.070	0.22	7.5	0.37
Chr6: 41,161,514:C:T	rs75932628	*TREM2*	*TREM2*-2	−0.29	0.20	0.16	8.3	0.36	−0.14	0.22	0.51	0	0.53
Chr7: 12,242,825:T:C	**rs7805419**	***TMEM106B***	***TMEM106B***	**0.065**	**0.018**	**3.1×10^{-4}**	27	0.21	**0.046**	**0.014**	**1.1×10^{-3}**	49	7.9×10^{-3}
Chr7: 100,386,466:T:C	rs2906657	*PILRA*	*PILRA*	−0.015	0.019	0.43	0	0.88	−0.014	0.015	0.34	40	0.036
Chr8: 27,362,470:C:T	rs73223431	*CLU*	*PTK2B*	0.036	0.018	0.042	0	0.58	0.041	0.014	4.2×10^{-3}	0.17	0.46
Chr8: 27,610,986:C:A	**rs867230**	***CLU***	***CLU***	**0.060**	**0.018**	**8.0×10^{-4}**	0	0.99	**0.051**	**0.014**	**2.8×10^{-4}**	0	0.49
Chr8: 144,103,704:G:A	**rs34173062**	***SHARPIN***	***SHARPIN***	−0.10	0.037	4.9×10^{-3}	47	0.080	**−0.098**	**0.029**	**7.8×10^{-4}**	15	0.29
Chr11: 60,173,126:T:A	rs7232	*MS4A6A*	*MS4A6A*	−0.030	0.019	0.11	44	0.087	−0.027	0.015	0.071	6.7	0.37
Chr11: 86,113,817:A:G	rs659023	*PICALM*	*PICALM*	0.045	0.018	0.015	13.	0.33	0.039	0.015	0.0071	46	0.020
Chr11: 121,564,878:T:C	rs11218343	*SORL1*	*SORL1*	−0.079	0.050	0.12	33.	0.16	−0.096	0.041	0.019	18	0.25
Chr14: 33,428,905:G:C	**rs187023552**	***NPAS3***	***NPAS3***	**−0.37**	**0.091**	**4.2×10^{-5}**	46	0.17	**−0.26**	**0.073**	**3.2×10^{-4}**	65	0.034
Chr14: 53,394,351:T:C	**rs10131116**	***FERMT2***	***DDHD1***	**−0.10**	**0.018**	**1.1×10^{-8}**	18.	0.29	**−0.069**	**0.014**	**1.2×10^{-6}**	32	0.088
Chr15: 58,790,588:T:G	rs347116	*ADAM10*	*ADAM10*	−0.034	0.018	0.068	0	0.74	−0.023	0.015	0.11	0	0.62
Chr15: 63,279,621:C:T	rs75763893	*APH1B*	*APH1B*	0.017	0.026	0.51	0	0.64	0.017	0.021	0.41	12	0.30
Chr15: 63,407,216:C:T	rs181364771	*APH1B*	*LINC02568*	−0.082	0.058	0.16	21	0.27	−0.067	0.047	0.15	30	0.12
Chr17: 44,352,876:C:T	rs5848	*GRN*	*GRN*	−0.041	0.019	0.030	0	0.86	−0.034	0.015	0.021	0	0.98
Chr17: 46,111,701:A:G	rs7225002	*MAPT*	*MAPT* H2	0.045	0.018	0.012	64	0.0075	0.032	0.014	0.025	34	0.066
Chr17: 63,470,201:G:A	rs8077276	*ACE*	*ACE*	0.031	0.018	0.088	0	0.82	0.028	0.014	0.048	0	0.82
Chr19: 1,050,875:A:G	rs12151021	*ABCA7*	*ABCA7*	−0.012	0.019	0.52	0	0.89	0.012	0.015	0.43	55	**1.6×10^{-3}**
Chr19: 54,304,006:C:T	rs1761453	*LILRA5*	*LILRA5*	−0.036	0.018	0.046	0	0.61	−0.032	0.014	0.023	0	0.62
Chr20: 56,449,045:G:A	rs113221226	*CASS4*	*CASS4*	−0.098	0.039	0.011	3.7	0.40	−0.058	0.031	0.061	2.9	0.42

Results of interaction testing with a dominant and an additive fixed-effect model on the summary data of the individual cohorts. The dominant model was a difference-of-effects analysis, while the additive model included the number of ε4 alleles. Significant interactions and *P* values ($P < 0.0017$) are in bold. [a]TOPMed r^2 identifier. [b]Reference SNP (rs) numbers, according to dbSNP build 156. [c]Nearest protein-coding or long intergenic nonprotein-coding RNA according to Ensembl release 111. [d]$\Delta\beta$ is calculated as $\beta_{43+44} - \beta_{33}$. [e]Two-sided raw *P* values were derived from a fixed-effect meta-analysis. [f]I^2 statistics, residual heterogeneity of the unaccounted variability. [g]Test for residual heterogeneity. [h]Effect per one ε4 allele.

https://doi.org/10.1038/s41588-026-02713-9

https://doi.org/10.1038/s41588-026-02713-9

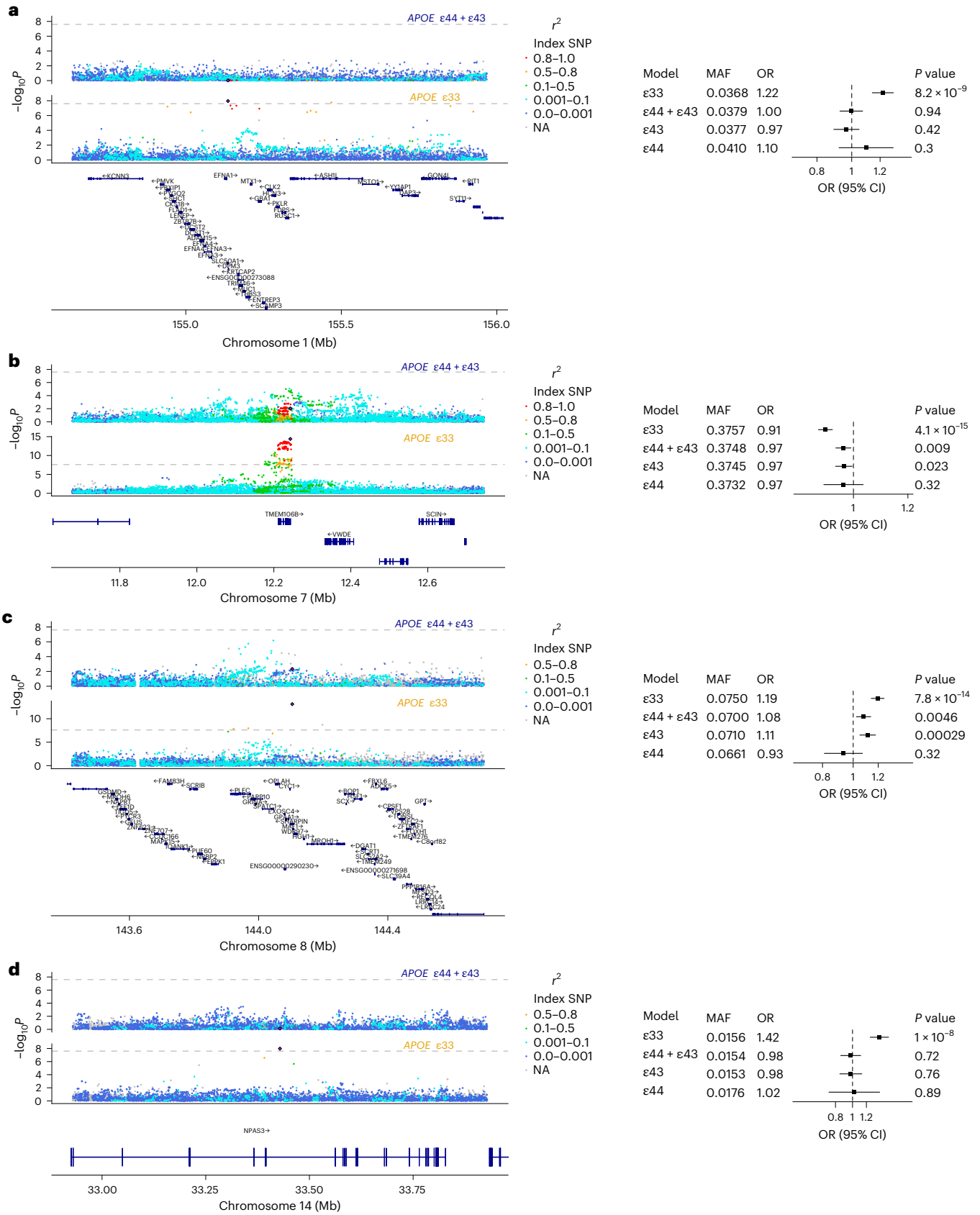


Fig. 2 | Locus and forest plots for the loci *SLC50A1*, *TMEM106B*, *SHARPIN* and *NPAS3* where the effect attenuates with the *APOE* ε4 allele. a–d, Locus plots for *SLC50A1* (**a**), *TMEM106B* (**b**), *SHARPIN* (**c**) and *NPAS3* (**d**) in *APOE* ε33 and *APOE* ε44 + ε43 strata. Forest plots of ORs for the lead SNPs in the four *APOE* strata ε33, ε44 + ε43, ε43 and ε44. In the forest plot, each *APOE* stratum is shown to visualize potential dominant or additive interaction. *P* values are raw two sided and were derived from a fixed-effect meta-analysis. The number of cases and controls in the respective stratified meta-analyses are shown in Supplementary Tables 3–6. MAF, minor allele frequency.

https://doi.org/10.1038/s41588-026-02713-9

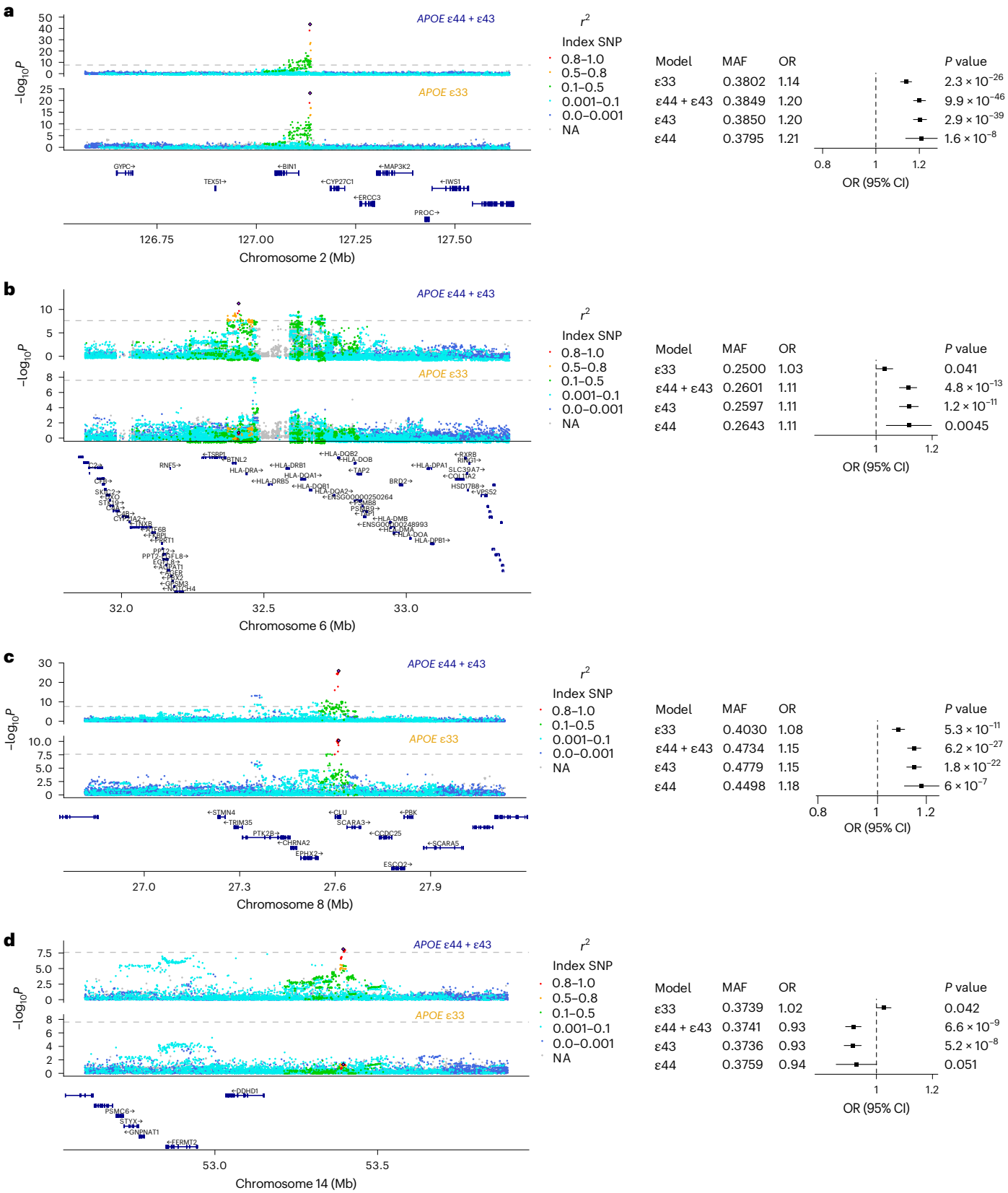


Fig. 3 | Locus and forest plots for the loci *BIN1*, *HLA-DRA*-1, *CLU* and *DDHD1* where the effect is augmented with the *APOE* ε4 allele. a–**d**, Locus plots for *BIN1* (**a**), *HLA-DRA*-1 (**b**), *CLU* (**c**) and *DDHD1* (**d**) in *APOE* ε33 and *APOE* ε44 + ε43 strata. Forest plots of ORs for the lead SNPs in the four *APOE* strata ε33, ε44 + ε43, ε43 and ε44. In the forest plot, each *APOE* stratum is shown to visualize potential dominant or additive interaction. *P* values are raw two sided and were derived from a fixed-effect meta-analysis. The number of cases and controls in the respective stratified meta-analyses are shown in Supplementary Tables 3–6.

https://doi.org/10.1038/s41588-026-02713-9

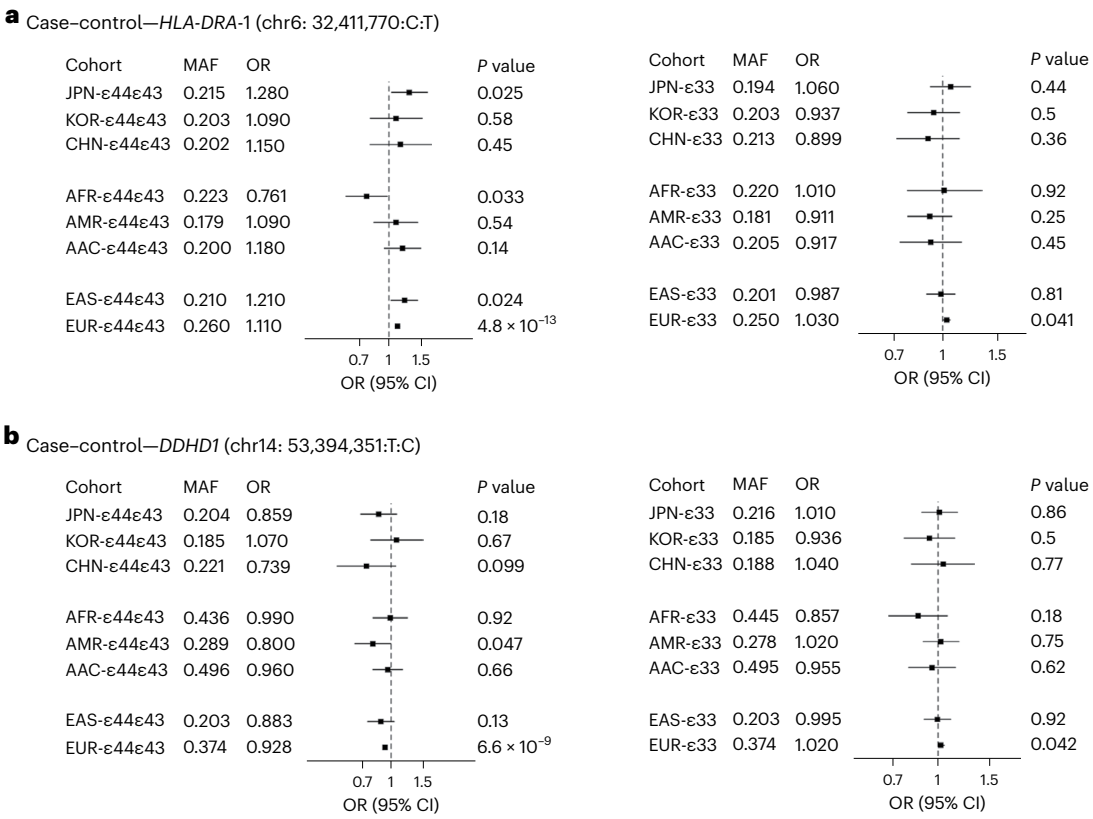


Fig. 4 | Multi-ancestry evaluation. a, Multi-ancestry results (ORs) for lead variant in *HLA-DRA* locus. **b**, Multi-ancestry results (ORs) for lead variant in *DDHD1* locus. *P* values are raw two sided and were derived from a fixed-effect meta-analysis. The number of cases and controls in the respective stratified meta-analyses are shown in Supplementary Table 12. CHN, Hong-Kong Chinese; JPN, Japanese; KOR, Korean; EAS, East Asian ancestry meta-analysis; EUR, European ancestry meta-analysis.

SLC50A1, *NPAS3* and *DDHD1*, discussed in detail in the paragraphs below. *HP1BP3* encodes heterochromatin protein 1 binding protein 3 and is a regulator of cell cycle progression[15]. *PTPRC* encodes protein tyrosine phosphatase receptor type C, also known as CD45, which is increasingly understood to have a role in the innate immune system[16,17]. *CHST9* encodes carbohydrate sulfotransferase 9, an enzyme that transfers sulfate to the position 4 of GalNAc. GalNAc4ST-1 and GalNAc4ST-2 transcripts are highly expressed in the pituitary gland and trachea[18,19]. *SMYD2* encodes a protein-lysine N-methyltransferase that methylates both histones and nonhistone proteins[20]. *PRAMEF1* encodes a protein PRAME family member 1 and has been associated with cancer (NCBI gene ID: 65121, www.ncbi.nlm.nih.gov/gene/65121). *GFRA1* encodes GDNF family receptor α-1, which is a receptor for both glial cell line-derived neurotrophic factor (GDNF) and neurturin (NTN), both potent neurotrophic factors and key regulators of neuron survival and differentiation (the Human Protein Atlas, www.proteinatlas.org)[21]. GDNF family receptor α-1 has been linked to the restoration of AD neuron survival[22].

The following genes were associated with attenuated effect sizes in ε4 carriers. *SLC50A1* is a new AD signal that only emerges in the *APOE* ε33 stratum and encodes solute carrier family 50 member 1, which is a sugar transporter for intercellular exchange and nutrition of pathogens[23]. The previously identified signal, *TMEM106B*[6], encodes the lysosomal type II transmembrane protein 106B, and residues of the protein have recently been shown to be amyloidogenic in an age-dependent manner and in several neurodegenerative diseases, including AD[24]. The presently identified lead hit is in the regulatory 3′ UTR part of the gene and is in full linkage disequilibrium (LD; $r^2 = 0.99$) with the previously reported rs1990622 variant, which is associated with reduced *TMEM106B* expression[25,26] and with earlier age at onset of frontotemporal lobar degeneration in *GRN* mutation carriers. Both the *TMEM106B* and *GRN* signals are sufficiently strong to reach genome-wide significance level in our previous overall GWAS[6]; however, the present *APOE*-stratified analyses illustrate that these signals only manifest in the *APOE* ε33 context, although only *TMEM106B* reached statistical significance in the stratified effect comparison test. Interestingly, *TMEM106B* and *GRN* were recently associated only with non-AD pathology in a comprehensive GWAS of multiple neuropathology endophenotypes of dementia[27]. Further aspects of pathophysiology are discussed in the Supplementary Note. *NPAS3* encodes a neuronal transcription factor implicated in several neuropsychiatric conditions[28] and is reported to have a regulatory function on the expression of reelin[29]. In adults, reelin binds to the ApoE-Receptor2 (apoER2) and the very low-density lipoprotein receptor, modulating AMPA and NMDA activities in the postsynaptic region, affecting amyloid precursor protein processing and tau hyperphosphorylation, and competing with apoE in receptor binding[30]. Furthermore, *SHARPIN* variants have been shown to affect NF-κB signaling in the nervous system, a central mediator of inflammatory and immune responses, and apoE is suggested to interact with NF-κB signaling[31,32]. In addition, we observed consistent directionality in all European ancestry cohorts, although the interaction test did not reach statistical significance, suggesting that the effect of *MAPT* is attenuated in an ε4 context, in agreement with a previous report[33]. Finally, forest plots of the effect differences for the significant stratified effect comparison tests show similar directionality across cohorts.

The following genes were associated with augmented effect sizes in ε4 carriers. The *HLA* region on chromosome 6 is highly complex. The present data add an extra layer to this complexity as we observed that one *HLA* locus associates with increased risk of AD in ε4 carriers, but not in ε3 carriers, while another independent *HLA* locus associates with

increased risk of AD in both strata. Furthermore, we confirmed *CLU* as one of the strongest genomic signals for AD and documented that this signal was substantially stronger in *APOE* ε4 carriers compared to ε33 carriers. We also identified a new independent signal within the *FERMT2* locus, where the nearest gene is *DDHD1* (distance 241,028 bp), which encodes a member of the phospholipase A1 family important in lipid and phospholipid metabolism[21] and is associated with a rare neuronal disease, spastic paraplegia 28 (refs. 34,35). The fact that the rs10131116 *DDHD1* variant in the present GWAS was associated with a decreased risk of AD specifically in *APOE* ε4 carriers, together with the recent identification of the rs10131116 as an eQTL associated with decreased *DDHD1* expression[6], highlights *DDHD1* as an interesting focus for drug discovery. *DDHD1* is also in the same biological pathway as a genome-wide significant known signal (*PLCG2*)[6]. Recently, *DDHD2*, a gene known to be involved in hereditary spastic paraplegia, was reported to provide flux of saturated fatty acids for neuronal energy and function[36], supporting a potential importance of this class of genes in neuronal functioning. Notably, the *HLA* and *DDHD1* signals were similar in European and Asian ancestry cohorts, despite differences in statistical power. Finally, forest plots of the effect differences also show similar directionality across cohorts.

By performing a large *APOE*-stratified GWAS, we have identified new as well as well-established AD loci, where the effect is manifested specifically in an *APOE* ε4 carrier or in an ε33 genotype context. These findings are supported by pathway analysis, highlighting distinct *APOE* carrier status-dependent biological mechanisms, and may have the potential to change our current understanding of the pathogenesis of AD. Based on our present findings and based on the observed less efficacy and higher risks of severe side effects in ε4 carriers in recent trials of anti-amyloid therapies, it may now be timely to consider including *APOE* stratification a priori in future randomized clinical trials of emerging AD medicines.

Online content

Any methods, additional references, Nature Portfolio reporting summaries, source data, extended data, supplementary information, acknowledgements, peer review information; details of author contributions and competing interests; and statements of data and code availability are available at https://doi.org/10.1038/s41588-026-02713-9.

References

1. Lambert, J.-C. et al. Meta-analysis of 74,046 individuals identifies 11 new susceptibility loci for Alzheimer's disease. *Nat. Genet.* **45**, 1452–1458 (2013).
2. Jansen, I. E. et al. Genome-wide meta-analysis identifies new loci and functional pathways influencing Alzheimer's disease risk. *Nat. Genet.* **51**, 404–413 (2019).
3. Kunkle, B. W. et al. Genetic meta-analysis of diagnosed Alzheimer's disease identifies new risk loci and implicates Aβ, tau, immunity and lipid processing. *Nat. Genet.* **51**, 414–430 (2019).
4. De Rojas, I. et al. Common variants in Alzheimer's disease: novel association of six genetic variants with AD and risk stratification by polygenic risk scores. *Nat. Commun.* **12**, 3417 (2021).
5. Wightman, D. P. et al. A genome-wide association study with 1,126,563 individuals identifies new risk loci for Alzheimer's disease. *Nat. Genet.* **53**, 1276–1282 (2021).
6. Bellenguez, C. et al. New insights into the genetic etiology of Alzheimer's disease and related dementias. *Nat. Genet.* **54**, 412–436 (2022).
7. Lambert, J. C., Ramirez, A., Grenier-Boley, B. & Bellenguez, C. Step by step: towards a better understanding of the genetic architecture of Alzheimer's disease. *Mol. Psychiatry* **28**, 2716–2727 (2023).
8. Corder, E. et al. Gene dose of apolipoprotein E type 4 allele and the risk of Alzheimer's disease in late onset families. *Science* **261**, 921–923 (1992).
9. Lake, J. et al. Multi-ancestry meta-analysis and fine-mapping in Alzheimer's disease. *Mol. Psychiatry* **28**, 3121–3132 (2023).
10. Fernandez-Calle, R. et al. *APOE* in the bullseye of neurodegenerative diseases: impact of the *APOE* genotype in Alzheimer's disease pathology and brain diseases. *Mol. Neurodegener.* **17**, 62 (2022).
11. Mintun, M. A. et al. Donanemab in early Alzheimer's disease. *N. Engl. J. Med.* **384**, 1691–1704 (2021).
12. Van Dyck, C. H. et al. Lecanemab in early Alzheimer's disease. *N. Engl. J. Med.* **388**, 9–21 (2023).
13. Sperling, R. A. et al. Trial of solanezumab in preclinical Alzheimer's disease. *N. Engl. J. Med.* **389**, 1096–1107 (2023).
14. GTEx Consortium. The GTEx Consortium atlas of genetic regulatory effects across human tissues. *Science* **369**, 1318–1330 (2020).
15. Dutta, B. et al. Profiling of the chromatin-associated proteome identifies HP1BP3 as a novel regulator of cell cycle progression. *Mol. Cell. Proteomics* **13**, 2183–2197 (2014).
16. Al Barashdi, M. A., Ali, A., McMullin, M. F. & Mills, K. Protein tyrosine phosphatase receptor type C (PTPRC or CD45). *J. Clin. Pathol.* **74**, 548–552 (2021).
17. Kaplan, R. et al. Cloning of three human tyrosine phosphatases reveals a multigene family of receptor-linked protein-tyrosine-phosphatases expressed in brain. *Proc. Natl Acad. Sci. USA* **87**, 7000–7004 (1990).
18. Kang, H.-G., Evers, M. R., Xia, G., Baenziger, J. U. & Schachner, M. Molecular cloning and expression of an N-acetylgalactosamine-4-O-sulfotransferase that transfers sulfate to terminal and non-terminal β1,4-linked N-acetylgalactosamine. *J. Biol. Chem.* **276**, 10861–10869 (2001).
19. Hiraoka, N., Misra, A., Belot, F., Hindsgaul, O. & Fukuda, M. Molecular cloning and expression of two distinct human N-acetylgalactosamine 4-O-sulfotransferases that transfer sulfate to GalNAcβ1→4GlcNAcβ1→R in both N- and O-glycans. *Glycobiology* **11**, 495–504 (2001).
20. Yi, X., Jiang, X. J. & Fang, Z. M. Histone methyltransferase SMYD2: ubiquitous regulator of disease. *Clin. Epigenetics* **11**, 112 (2019).
21. Sjostedt, E. et al. An atlas of the protein-coding genes in the human, pig, and mouse brain. *Science* **367**, eaay5947 (2020).
22. Konishi, Y. et al. Deficiency of GDNF receptor GFRα1 in Alzheimer's neurons results in neuronal death. *J. Neurosci.* **34**, 13127–13138 (2014).
23. Chen, L. Q. et al. Sugar transporters for intercellular exchange and nutrition of pathogens. *Nature* **468**, 527–532 (2010).
24. Schweighauser, M. et al. Age-dependent formation of *TMEM106B* amyloid filaments in human brains. *Nature* **605**, 310–314 (2022).
25. Cruchaga, C. et al. Association of *TMEM106B* gene polymorphism with age at onset in granulin mutation carriers and plasma granulin protein levels. *Arch. Neurol.* **68**, 581–586 (2011).
26. Van Deerlin, V. M. et al. Common variants at 7p21 are associated with frontotemporal lobar degeneration with TDP-43 inclusions. *Nat. Genet.* **42**, 234–239 (2010).
27. Shade, L. M. P. et al. GWAS of multiple neuropathology endophenotypes identifies new risk loci and provides insights into the genetic risk of dementia. *Nat. Genet.* **56**, 2407–2421 (2024).
28. Michaelson, J. J. et al. Neuronal PAS domain proteins 1 and 3 are master regulators of neuropsychiatric risk genes. *Biol. Psychiatry* **82**, 213–223 (2017).
29. Erbel-Sieler, C. et al. Behavioral and regulatory abnormalities in mice deficient in the NPAS1 and NPAS3 transcription factors. *Proc. Natl Acad. Sci. USA* **101**, 13648–13653 (2004).
30. Stranahan, A. M., Erion, J. R. & Wosiski-Kuhn, M. Reelin signaling in development, maintenance, and plasticity of neural networks. *Ageing Res. Rev.* **12**, 815–822 (2013).

31. Asanomi, Y. et al. A rare functional variant of *SHARPIN* attenuates the inflammatory response and associates with increased risk of late-onset Alzheimer's disease. *Mol. Med.* **25**, 20 (2019).
32. Arnaud, L. et al. APOE4 drives inflammation in human astrocytes via TAGLN3 repression and NF-κB activation. *Cell Rep.* **40**, 111200 (2022).
33. Jun, G. et al. A novel Alzheimer disease locus located near the gene encoding tau protein. *Mol. Psychiatry* **21**, 108–117 (2016).
34. Bouslam, N. et al. Mapping of a new form of pure autosomal recessive spastic paraplegia (SPG28). *Ann. Neurol.* **57**, 567–571 (2005).
35. Tesson, C. et al. Alteration of fatty-acid-metabolizing enzymes affects mitochondrial form and function in hereditary spastic paraplegia. *Am. J. Hum. Genet.* **91**, 1051–1064 (2012).
36. Saber, S. H. et al. *DDHD2* provides a flux of saturated fatty acids for neuronal energy and function. *Nat. Metab.* **7**, 2117–2141 (2025).

Publisher's note Springer Nature remains neutral with regard to jurisdictional claims in published maps and institutional affiliations.

Open Access This article is licensed under a Creative Commons Attribution-NonCommercial-NoDerivatives 4.0 International License, which permits any non-commercial use, sharing, distribution and reproduction in any medium or format, as long as you give appropriate credit to the original author(s) and the source, provide a link to the Creative Commons licence, and indicate if you modified the licensed material. You do not have permission under this licence to share adapted material derived from this article or parts of it. The images or other third party material in this article are included in the article's Creative Commons licence, unless indicated otherwise in a credit line to the material. If material is not included in the article's Creative Commons licence and your intended use is not permitted by statutory regulation or exceeds the permitted use, you will need to obtain permission directly from the copyright holder. To view a copy of this licence, visit http://creativecommons.org/licenses/by-nc-nd/4.0/.

© The Author(s) 2026

Jesper Qvist Thomassen[1,160] ✉, Hampton Leonard[2,160], Brittany Ulms[3,160], Benjamin Grenier-Boley[4,160], Sami Heikkinen[5,160], Pablo Garcia-González[6,7,8,160], Atahualapa Castillo-Morales[9], Masataka Kikuchi[10], Jungsoo Gim[11,12,13,14], Han Cao[15,16], Fahri Küçükali[17,18], Najaf Amin[3], Dabin Yoon[11,12], Itziar de Rojas[6,7,19], Pilar Alvarez Jerez[2], Victoria Alvarez[20,21], Beatrice Arosio[22,23], Céline Bellenguez[4], Sverre Bergh[24,25], Kimberley Billingsley[2], Cornelis Blauwendraat[26], Merce Boada[6,7], Barbara Borroni[27,28], Paola Bossù[29], María J. Bullido[7,30,31], Antonio Daniele[32,33], Ángel Carracedo[34,35], Alexandre de Mendonça[36], Mark Cookson[2], Jürgen Deckert[37], Martin Dichgans[38,39,40], Srdjan Djurovic[41,42], Oriol Dols-Icardo[7,43], Carole Dufouil[44], Emrah Düzel[45,46], Valentina Escott-Price[47], Tormod Fladby[48,49], Laura Fratiglioni[50,51], Amy K. Y. Fu[15,16,52,53], Daniela Galimberti[54,55], Jose Maria García-Alberca[7,56], Vilmantas Giedraitis[57], Guillermo Garcia-Ribas[58], Caroline Graff[50,51], Timo Grimmer[59], Edna Grünblatt[60,61,62], Olivier Hanon[63], Lucrezia Hausner[64], Stefanie Heilmann-Heimbach[65], Jakub Hort[66,67], Frank Jessen[68,69,70], Kendall Jensen[71], Caroline Jonson[2], Yoontae Kim[12,13], Nicole Kuznetsov[2], Ville Leinonen[72,73], Anssi Lipponen[5], Jiao Luo[1,74], Mary Makarious[2], Henna Martiskainen[5], Carlo Masullo[75], Patrizia Mecocci[76,77], Shima Mehrabian[78], Pablo Mir[7,79,80], Akinori Miyashita[10], Susanne Moebus[81], Kin Y. Mok[15,16,82], Laura Molina Porcel[83,84], Fermin Moreno[7,85,86], Benedetta Nacmias[87,88], Lucilla Parnetti[89], Pau Pastor[90,91], Jordi Pérez-Tur[7,92], Oliver Peters[93,94], Yolande A. L. Pijnenburg[95,96], Gerard Piñol-Ripoll[97,98], Julius Popp[99,100,101], Innocenzo Rainero[102], Luis M. Real[103,104], Steffi Riedel-Heller[105], Eloy Rodriguez-Rodriguez[7,106], Arvid Rongve[107], Giacomina Rossi[108], Jose Luis Royo[104], Dan Rujescu[109,110], Ingvild Saltvedt[111], María Eugenia Sáez[112], Raquel Sánchez-Valle[113], Florentino Sanchez-Garcia[114], Nicolai Sandau[1], Nikolaos Scarmeas[115,116], Katja Scheffler[111,117], Norbert Scherbaum[118], Anja Schneider[69,119], Geir Selbæk[120,121,122], Davide Seripa[123], Vincenzo Solfrizzi[124,125], Marco Spallazzi[126], Alessio Squassina[127], Eystein Stordal[128], Niccoló Tesi[96,129,130], Lucio Tremolizzo[131,132], Kumar P. Tripathi[133,134], Wiesje M. van der Flier[95,96,135], Julie Williams[9,136], Jens Wiltfang[137,138,139], Dag Aarsland[140,141,142], Andrew B. Singleton[2], Philippe Amouyel[4], Stéphanie Debette[44], Magda Tsolaki[143,144,145], Gael Nicolas[146], Sven van der Lee[95,96,129], Henne Holstege[95,96,129,147,148], Maria Victoria Fernandez[6], Patrick Gavin Kehoe[149], Kristel Sleegers[17,18], Martin Ingelsson[57,150,151], Roberta Ghidoni[28], Ole A. Andreassen[42,152,153], Peter A. Holmans[136], Pascual Sánchez-Juan[7,154], Rebecca Sims[136], Nancy Y. Ip[15,16,52,53], Kun Ho Lee[11,13,14,155], Takeshi Ikeuchi[10], Alfredo Ramirez[69,70,119,133,156], Agustin Ruiz[6,7,157], Mikko Hiltunen[5,161], Jean-Charles Lambert[4,161], Cornelia van Duijn[3,158,161], Mike Nalls[2,161] ✉ & Ruth Frikke-Schmidt[1,159,161] ✉

[1]Department of Clinical Biochemistry, Copenhagen University Hospital—Rigshospitalet, Copenhagen, Denmark. [2]Center for Alzheimer's and Related Dementias, National Institute on Aging, Bethesda, MD, USA. [3]Nuffield Department of Population Health, University of Oxford, Oxford, UK. [4]Université de Lille, Inserm, CHU Lille, Institut Pasteur de Lille, Lille, France. [5]Institute of Biomedicine, University of Eastern Finland, Kuopio, Finland. [6]Ace Alzheimer Center Barcelona, Universitat Internacional de Catalunya (UIC), Barcelona, Spain. [7]Network Center on Biomedical Research in Neurodegenerative Diseases (CIBERNED), National Institute of Health Carlos III, Madrid, Spain. [8]PhD Program in Biotechnology, Faculty of Pharmacy and Food Sciences, University of Barcelona, Barcelona, Spain. [9]UK Dementia Research Institute, School of Medicine, Cardiff University, Cardiff, UK. [10]Department of Molecular Genetics, Brain Research Institute, Niigata University, Niigata, Japan. [11]Department of Biomedical Science, Chosun University, Gwangju, Republic of Korea. [12]Well-aging Medicare Institute & CSU G-LAMP Project Group, Chosun University, Gwangju, Republic of Korea. [13]BK FOUR Department of Integrative Biological Sciences, Chosun University, Gwangju, Republic of Korea. [14]Gwangju Alzheimer's & Related Dementia (GARD) Cohort Research Center, Chosun University, Gwangju, Republic of Korea. [15]Division of Life Science, State Key Laboratory of Molecular Neuroscience and Daniel and Mayce Yu Molecular

Neuroscience Center, The Hong Kong University of Science and Technology, Hong Kong, China. [16]Hong Kong Center for Neurodegenerative Diseases, InnoHK, Hong Kong, China. [17]VIB Center for Molecular Neurology, VIB, Antwerp, Belgium. [18]Department of Biomedical Sciences, University of Antwerp, Antwerp, Belgium. [19]Luxembourg Centre for Systems Biomedicine (LCSB), University of Luxembourg, Esch-sur-Alzette, Luxembourg. [20]Laboratorio de Genética, Hospital Universitario Central de Asturias, Oviedo, Spain. [21]Instituto de Investigación Sanitaria del Principado de Asturias (ISPA), Oviedo, Spain. [22]Department of Clinical Sciences and Community Health, University of Milan, Milan, Italy. [23]Geriatric Unit, Fondazione IRCCS Ca' Granda Ospedale Maggiore Policlinico, Milan, Italy. [24]The Research Centre for Age-related Functional Decline and Disease, Innlandet Hospital Trust, Ottestad, Norway. [25]Norwegian National Centre for Aging and Health, Vestfold Health Trust, Tønsberg, Norway. [26]Coalition for Aligning Science, Chevy Chase, MD, USA. [27]Department of Clinical and Experimental Sciences, University of Brescia, Brescia, Italy. [28]Molecular Markers Laboratory, IRCCS Istituto Centro San Giovanni di Dio Fatebenefratelli, Brescia, Italy. [29]Laboratory of Experimental Neuropsychobiology, Clinical Neuroscience and Neurorehabilitation Department, IRCCS Santa Lucia Foundation, Rome, Italy. [30]Centro de Biología Molecular Severo Ochoa (UAM-CSIC), Madrid, Spain. [31]Instituto de Investigacion Sanitaria 'Hospital la Paz' (IdIPaz), Madrid, Spain. [32]Department of Neuroscience, Università Cattolica del Sacro Cuore, Rome, Italy. [33]Neurology Unit, IRCCS Fondazione Policlinico Universitario A. Gemelli, Rome, Italy. [34]Grupo de Medicina Xenómica, CIBERER, CIMUS, Universidade de Santiago de Compostela, Santiago de Compostela, Spain. [35]Fundación Pública Galega de Medicina Xenómica—IDIS, Santiago de Compostela, Spain. [36]Faculty of Medicine, University of Lisbon, Lisbon, Portugal. [37]Department of Psychiatry, Psychosomatics and Psychotherapy, Center of Mental Health, University Hospital of Würzburg, Würzburg, Germany. [38]Institute for Stroke and Dementia Research (ISD), University Hospital, LMU Munich, Munich, Germany. [39]German Center for Neurodegenerative Diseases (DZNE), Munich, Germany. [40]Munich Cluster for Systems Neurology (SyNergy), Munich, Germany. [41]Department of Medical Genetics, Oslo University Hospital, Oslo, Norway. [42]Centre for Precision Psychiatry, Institute of Clinical Medicine, University of Oslo, Oslo, Norway. [43]Department of Neurology, Institut de Recerca Sant Pau, Hospital de la Santa Creu i Sant Pau, Universitat Autònoma de Barcelona, Barcelona, Spain. [44]University of Bordeaux, Inserm Bordeaux Population Health Research Center U1219, Bordeaux, France. [45]German Center for Neurodegenerative Diseases (DZNE), Magdeburg, Germany. [46]Institute of Cognitive Neurology and Dementia Research (IKND), Otto-von-Guericke University, Magdeburg, Germany. [47]UKDRI@ Cardiff, School of Medicine, Cardiff University, Cardiff, UK. [48]Institute of Clinical Medicine, Campus Ahus, University of Oslo, Oslo, Norway. [49]Department of Neurology, Akershus University Hospital, Lørenskog, Norway. [50]Karolinska University Hospital, Theme inflammation and Aging, Stockholm, Sweden. [51]Department of NVS, Center for Alzheimer Research, Karolinska Institutet, Stockholm, Sweden. [52]Guangdong Provincial Key Laboratory of Brain Science, Disease and Drug Development, HKUST Shenzhen Research Institute, Shenzhen, China. [53]SIAT-HKUST Joint Laboratory for Brain Science, Shenzhen, China. [54]Neurodegenerative Diseases Unit, Fondazione IRCCS Ca' Granda, Ospedale Policlinico, Milan, Italy. [55]Department of Biomedical, Surgical and Dental Sciences, University of Milan, Milan, Italy. [56]Alzheimer Research Center & Memory Clinic, Andalusian Institute for Neuroscience, Málaga, Spain. [57]Department of Public Health and Caring Sciences, Clinical Geriatrics, Uppsala University, Uppsala, Sweden. [58]Hospital Universitario Ramon y Cajal, IRYCIS, Madrid, Spain. [59]Center for Cognitive Disorders, Department of Psychiatry and Psychotherapy, Technical University of Munich, School of Medicine, Munich, Germany. [60]Department of Child and Adolescent Psychiatry and Psychotherapy, University Hospital of Psychiatry Zurich, University of Zurich, Zurich, Switzerland. [61]Neuroscience Center Zurich, University of Zurich and ETH Zurich, Zurich, Switzerland. [62]Zurich Center for Integrative Human Physiology, University of Zurich, Zurich, Switzerland. [63]Université Paris Cité, EA 4468, APHP, Hospital Broca, Memory Resource and Research Centre of de Paris-Broca-Ile de France, Paris, France. [64]Department of Geriatric Psychiatry, Central Institute for Mental Health Mannheim, Faculty Mannheim, University of Heidelberg, Mannheim, Germany. [65]Institute of Human Genetics, University of Bonn, School of Medicine & University Hospital Bonn, Bonn, Germany. [66]Memory Clinic, Department of Neurology, Charles University, Second Faculty of Medicine and Motol University Hospital, Prague, Czech Republic. [67]International Clinical Research Center, St. Anne's University Hospital Brno, Brno, Czech Republic. [68]Department of Psychiatry and Psychotherapy, Faculty of Medicine and University Hospital Cologne, University of Cologne, Cologne, Germany. [69]German Center for Neurodegenerative Diseases (DZNE), Bonn, Germany. [70]Cologne Cluster of Excellence on Aging in Aging-Associated Diseases (CECAD), University of Cologne, Cologne, Germany. [71]Center for Noninvasive Diagnostics, TGen, Phoenix, AZ, USA. [72]Department of Neurosurgery, Kuopio University Hospital, Kuopio, Finland. [73]Institute of Clinical Medicine-Neurosurgery, University of Eastern Finland, Kuopio, Finland. [74]Novo Nordisk Foundation Center for Basic Metabolic Research, Faculty of Health and Medical Science, University of Copenhagen, Copenhagen, Denmark. [75]Institute of Neurology, Catholic University of the Sacred Heart, Rome, Italy. [76]Division of Gerontology and Geriatrics, Department of Medicine and Surgery, University of Perugia, Perugia, Italy. [77]Division of Clinical Geriatrics, Department of Neurobiology, Care Sciences and Society, Karolinska Institutet, Stockholm, Sweden. [78]Clinic of Neurology, UH 'Alexandrovska', Medical University—Sofia, Sofia, Bulgaria. [79]Unidad de Trastornos del Movimiento, Servicio de Neurología y Neurofisiología, Instituto de Biomedicina de Sevilla (IBiS), Hospital Universitario Virgen del Rocío/CSIC/Universidad de Sevilla, Seville, Spain. [80]Departamento de Medicina, Facultad de Medicina, Universidad de Sevilla, Seville, Spain. [81]Institute for Urban Public Health, University Hospital of University Duisburg-Essen, Essen, Germany. [82]Department of Molecular Neuroscience, UCL Institute of Neurology, London, UK. [83]Neurological Tissue Bank—Biobanc—Hospital Clinic—IDIBAPS, Barcelona, Spain. [84]Alzheimer's Disease and Other Cognitive Disorders Unit, Neurology Department, Hospital Clinic, Barcelona, Spain. [85]Department of Neurology, Hospital Universitario Donostia, San Sebastian, Spain. [86]Neurosciences Area, Instituto Biodonostia, San Sebastian, Spain. [87]Department of Neuroscience, Psychology, Drug Research and Child Health, University of Florence, Florence, Italy. [88]IRCCS Fondazione Don Carlo Gnocchi, Florence, Italy. [89]Centre for Memory Disturbances, Lab of Clinical Neurochemistry, Section of Neurology, University of Perugia, Perugia, Italy. [90]Fundació Docència i Recerca Mútua Terrassa, Barcelona, Spain. [91]Memory Disorders Unit, Department of Neurology, Hospital Universitari Mutua de Terrassa, Barcelona, Spain. [92]Unitat de Genètica Molecular, Institut de Biomedicina de València-CSIC, Valencia, Spain. [93]German Center for Neurodegenerative Diseases (DZNE), Berlin, Germany. [94]Charité—Universitätsmedizin Berlin, Freie Universität Berlin, Humboldt-Universität zu Berlin, and Berlin Institute of Health, Institute of Psychiatry and Psychotherapy, Berlin, Germany. [95]Alzheimer Center Amsterdam, Neurology, Vrije Universiteit Amsterdam, Amsterdam UMC Location VUmc, Amsterdam, the Netherlands. [96]Amsterdam Neuroscience, Neurodegeneration, Amsterdam, the Netherlands. [97]Unitat Trastorns Cognitius, Hospital Universitari Santa Maria de Lleida, Lleida, Spain. [98]Institut de Recerca Biomedica de Lleida (IRBLLeida), Lleida, Spain. [99]Old Age Psychiatry, Department of Psychiatry, Lausanne University Hospital, Lausanne, Switzerland. [100]Department of Geriatric Psychiatry, University Hospital of Psychiatry Zürich, Zürich, Switzerland. [101]Institute for Regenerative Medicine, University of Zürich, Zürich, Switzerland. [102]Department of Neuroscience 'Rita Levi Montalcini', University of Torino, Torino, Italy. [103]Unidad Clínica de Enfermedades Infecciosas y Microbiología, Hospital Universitario de Valme, Sevilla, Spain. [104]Depatamento de Especialidades Quirúrgicas, Bioquímica e Inmunología, Facultad de Medicina, Universidad de Málaga, Málaga, Spain. [105]Institute of Social Medicine, Occupational Health and Public Health, University of Leipzig, Leipzig, Germany. [106]Neurology Service, Marqués de Valdecilla University Hospital (University of Cantabria and IDIVAL), Santander, Spain. [107]Department of Research and Innovation, Haugesund Hospital, Haugesund, Norway. [108]Unit of Neurology V—Neuropathology, Fondazione IRCCS Istituto Neurologico Carlo Besta, Milan, Italy. [109]Department of Psychiatry and Psychotherapy, Medical University Vienna, Vienna, Austria. [110]Martin-Luther-University Halle-Wittenberg, University Clinic and Outpatient Clinic for Psychiatry, Psychotherapy and

Psychosomatics, Halle (Saale), Germany. [111]Department of Neuromedicine and Movement Science, Faculty of Medicine and Health Sciences, Norwegian University of Science and Technology (NTNU), Department of Geriatrics, St. Olav's Hospital, Trondheim University Hospital, Trondheim, Norway. [112]CAEBI, Centro Andaluz de Estudios Bioinformáticos, Sevilla, Spain. [113]Alzheimer's Disease and Other Cognitive Disorders Unit, Service of Neurology, Hospital Clínic of Barcelona, Institut d'Investigacions Biomèdiques August Pi i Sunyer, University of Barcelona, Barcelona, Spain. [114]Department of Immunology, Hospital Universitario Doctor Negrín, Las Palmas, Spain. [115]Taub Institute for Research in Alzheimer's Disease and the Aging Brain, The Gertrude H. Sergievsky Center, Depatment of Neurology, Columbia University, New York City, NY, USA. [116]First Department of Neurology, Aiginition Hospital, National and Kapodistrian University of Athens, Medical School, Athens, Greece. [117]Department of Neurology and Clinical Neurophysiology, Trondheim University Hospital, Trondheim, Norway. [118]Department of Psychiatry and Psychotherapy, LVR-Klinikum Essen, University of Duisburg-Essen, Essen, Germany. [119]Department for Cognitive Disorders and Old Age Psychiatry, University Hospital Bonn, Bonn, Germany. [120]Norwegian National Advisory Unit on Aging and Health, Vestfold Health Trust, Tønsberg, Norway. [121]Institute of Health and Society, Faculty of Medicine, University of Oslo, Oslo, Norway. [122]Centre for Old Age Psychiatric Research, Innlandet Hospital Trust, Ottestad, Norway. [123]Department of Hematology and Stem Cell Transplant, Vito Fazzi Hospital, Lecce, Italy. [124]Interdisciplinary Department of Medicine, Geriatric Medicine and Memory Unit, University of Bari Aldo Moro, Bari, Italy. [125]Academic Division 'C. Frugoni' & Hospital Division of Internal and Geriatric Medicine, Policlinico Hospital, Bari, Italy. [126]Department of Medicine and Surgery, Unit of Neurology, University-Hospital of Parma, Parma, Italy. [127]Department of Biomedical Sciences, Section of Neuroscience and Clinical Pharmacology, University of Cagliari, Cagliari, Italy. [128]Namsos Hospital, Namsos, Norway. [129]Genomics of Neurodegenerative Diseases and Aging, Human Genetics, Vrije Universiteit Amsterdam, Amsterdam UMC Location VUmc, Amsterdam, the Netherlands. [130]Delft Bioinformatics Lab, Delft University of Technology, Delft, the Netherlands. [131]Neurology Unit, IRCCS 'San Gerardo dei Tintori', Monza, Italy. [132]School of Medicine and Surgery, University of Milano-Bicocca, Monza, Italy. [133]Division of Neurogenetics and Molecular Psychiatry, Department of Psychiatry and Psychotherapy, Faculty of Medicine and University Hospital Cologne, University of Cologne, Cologne, Germany. [134]Estudios en Neurociencias y Sistemas Complejos (ENyS) CONICET-HEC-UNAJ, Buenos Aires, Argentina. [135]Epidemiology and Data Science, Vrije Universiteit Amsterdam, Amsterdam UMC Location VUmc, Amsterdam, the Netherlands. [136]Division of Psychological Medicine and Clinical Neuroscience, School of Medicine, Cardiff University, Cardiff, UK. [137]Department of Psychiatry and Psychotherapy, University Medical Center Goettingen, Goettingen, Germany. [138]German Center for Neurodegenerative Diseases (DZNE), Goettingen, Germany. [139]Medical Science Department, iBiMED, Aveiro, Portugal. [140]Department of Old Age Psychiatry, Division of Academic Psychiatry, Institute of Psychiatry, Psychology and Neuroscience, King's College London, London, UK. [141]Wolfson Centre for Age Related Diseases, Division of Neuroscience of the Institute of Psychiatry, Psychology and Neuroscience, King's College London, London, UK. [142]Stavanger University Hospital, Stavanger, Norway. [143]1st Department of Neurology, Medical School, Aristotle University of Thessaloniki, Thessaloniki, Greece. [144]Laboratory of Neurodegenerative Diseases, Center for Interdisciplinary Research and Innovation (CIRI—AUTh), Balkan Center, Aristotle University of Thessaloniki, Thessaloniki, Greece. [145]Greek Alzheimer Disease Association and Related Disorders, Thessaloniki, Greece. [146]Univ Rouen Normandie, Normandie Univ, Inserm U1245 and CHU Rouen, Department of Genetics and Reference Center for Developmental Disorders, Rouen, France. [147]VIB Center for Brain and Disease Research, Leuven, Belgium. [148]Department of Neurosciences, Leuven Brain Institute, KU Leuven, Leuven, Belgium. [149]Bristol Medical School, University of Bristol, Bristol, UK. [150]Krembil Brain Institute, University Health Network, Toronto, Ontario, Canada. [151]Tanz Centre for Research in Neurodegenerative Diseases, Departments of Medicine and Laboratory Medicine & Pathobiology, University of Toronto, Toronto, Ontario, Canada. [152]Division of Mental Health and Addiction, Oslo University Hospital, Oslo, Norway. [153]KG Jebsen Centre for Neurodevelopmental disorders, University of Oslo, Oslo, Norway. [154]Alzheimer's Centre Reina Sofia-CIEN Foundation, Madrid, Spain. [155]Department of Neural Development and Disease, Korea Brain Research Institute, Daegu, Korea. [156]Department of Psychiatry and Glenn Biggs Institute for Alzheimer's and Neurodegenerative Diseases, UT Health San Antonio, San Antonio, TX, USA. [157]Biggs Institute for Alzheimer's and Neurodegenerative Diseases, University of Texas Health Science Center, San Antonio, TX, USA. [158]Department of Epidemiology, ErasmusMC, Rotterdam, the Netherlands. [159]Department of Clinical Medicine, Faculty of Health and Medical Sciences, University of Copenhagen, Copenhagen, Denmark. [160]These authors contributed equally: Jesper Qvist Thomassen, Hampton Leonard, Brittany Ulms, Benjamin Grenier-Boley, Sami Heikkinen, Pablo Garcia-González. [161]These authors jointly supervised this work: Mikko Hiltunen, Jean-Charles Lambert, Cornelia van Duijn, Mike Nalls & Ruth Frikke-Schmidt. ✉e-mail: jesper.qvist.thomassen@regionh.dk; mike@datatecnica.com; ruth.frikke-schmidt@regionh.dk

Methods

Populations

We used the following European ancestry consortia/biobanks: European Alzheimer's Disease & Dementia BioBank (EADB), FinnGen, European Alzheimer's Disease Initiative, Bonn, Genome Research at Fundacio ACE (Gr@CE), Genetic and Environmental Risk in Alzheimer's Disease, Alzheimer's Disease Sequencing Project (ADSP) and UK Biobank (UKB). In addition, we evaluated 33 regions of interest in cohorts of East Asian (EAS) ancestry, representing Japanese (JADNI, CL, NP; EAS-JPN), Chinese (HKS; EAS-CHN) and Korean (GARD; EAS-KOR) populations, as well as in AAC (ADSP-AAC), AFR (ADSP-AFR) and native AMR (ADSP-AMR) multi-ancestry populations. *APOE* genotype was determined by the imputed data using rs7412 and rs429358. Where directly genotyped data were available, samples with a mismatch between the imputed and genotyped *APOE* genotype were excluded. FinnGen R11 was used, excluding samples from the ADGEN study as they are embedded in the EADB. AD cases were defined by diagnosis or by the use of AD medication (ATC code: N06D). Individuals diagnosed with other forms of dementia were excluded from the controls, and all individuals with an AD diagnosis were included independent of other dementia diagnoses. In UKB only, those defined as white British were included, and AD was defined as being diagnosed with AD from electronic medical records. No information regarding proxies was used in the AD definition or as exclusion criteria. In all datasets, controls younger than 60 years were excluded to better balance the age distributions in the cases and controls and to avoid the inclusion of young controls. All cases were kept. Written informed consent was obtained from study participants or, for those with substantial cognitive impairment, a caregiver, legal guardian or other proxy. Study protocols for all cohorts were reviewed and approved by the appropriate institutional review boards.

Quality control (QC) and imputation

A standard QC was performed on the samples and variants in all datasets. The samples were imputed using TOPMed except for ADSP and FinnGen (Supplementary Table 2). FinnGen was imputed with a Finnish whole-genome sequencing reference panel (SiSu; v4). Ancestry estimates and QC for UKB and ADSP were done using GenoTools[37].

GWAS analysis

Test of the association between clinical AD status and autosomal genetic variants was conducted separately in each cohort by means of logistic regression or mixed models using an additive genetic model. Three software implementations were used (SNPTEST (v2.5.6), PLINK2 and REGENIE)[38–40] and adjusted for sex, age, genetic principal components (gPCs) and genotyping centers/batches when necessary (Supplementary Table 2). gPCs were calculated in the full cohort and not in the individual strata to avoid generating possible ascertainment bias effects. Sensitivity analyses were carried out in some datasets to check that adjusting for age did not introduce spurious findings. In SNPTEST, we analyzed the genotype probabilities using the newml method. In PLINK2 and REGENIE, dosages were used combined with the glm regression (Firth's regression if failed convergence) in PLINK2 and Firth's regression in REGENIE. For each dataset, we filtered out variants with (1) missing data on the effect size, s.e. or *P* value, (2) an absolute effect above 5, (3) an imputation quality below 0.3 and (4) variants not fulfilling $2 \times \min(n_{cases}, n_{controls}) \times$ minor allele frequency $\times$ info > 5 (an unbalanced MAC-info score), where info is imputation quality. A fixed-effect meta-analysis using an inverse-variance weighted approach as implemented in METAL (v2020-05-05) was performed combining the results from each dataset. Variants were excluded if a heterogeneity *P* value was below 5×10^{-8} or if variants did not pass QC in at least two of the three major datasets (EADB TOPMed, FinnGen, UKB). The genomic inflation factor was computed with a median approach after the exclusion of the *APOE* region (44–46 Mb on chromosome 19 in GRCh38) both for variants with minor allele frequency of >1% and in the entire dataset. Manhattan plots were made using topr package[41] (v2.0.2) in R (v4.3.3).

Definition of loci

Around each variant with a *P* value below 2.5×10^{-8}, a region of ±500 kb was defined per fixed-effect meta-analysis. Most of the variants will be highly correlated across the strata except for those variants that interact with the *APOE* genotype, which is expected to be a small minority of the total tested variants. Hence, if one were to consider all GWAS tests as belonging to the same family, it would lead to a large increase in risk of type II errors without much gain in controlling for type I errors. To determine the proper control of multiple testing, the effective number of independent tests (M_{eff}) was determined using the Li & Ji eigenvalue decomposition[42] of the interstratum effect estimate correlation matrix. Summary statistics from ε44, ε43, ε44 + ε43 and ε33 strata were merged, and the SNPs were thinned to one per 500-kb (or 250-kb) window, retaining the SNP with the lowest combined *P* value, excluding the *APOE* region (chr19: 40–50 Mb). M_{eff} was estimated across signal enrichment thresholds from $|z| = 0$ to 7. M_{eff} decreased from 2.6 at $|z| = 0$ (noise dominated, $\beta = 0$) and plateaued at 1.3–1.4 for $|z| > 5$ (Supplementary Fig. 85), consistent with one shared genetic dimension and a partial second dimension corresponding to the ε4-interacting minority of loci. However, to be conservative in setting a *P*-value threshold for the stratified GWAS analysis, we set a stricter multiple testing correction of $M_{eff} = 2$ instead of $M_{eff,Li\&Ji} = 1.4$, resulting in the threshold $P < 5 \times 10^{-8}/2 = 2.5 \times 10^{-8}$. We used the PLINK2 clumping procedure to define independent signals in each region. This procedure is iterative, starting with the variant with the lowest *P* value in the respective region (the lead SNP). All variants within loci and in LD with the lead variant (r^2 higher than 0.01) are assigned to the clump belonging to the lead SNP. If any variant with a *P* value below 2.5×10^{-8} is unassigned to a clump in the respective region, the variant with the lowest *P* value is found among the remaining variants, and the clumping is repeated until all variants have been assigned a clump. LD in the EADB TOPMed imputed dataset was computed using high-quality imputed dosages (imputation info > 0.8). The clumping procedure was run in both the ε44 + ε43 and ε33 GWAS results, and the results for the respective loci were compared. Loci plots were generated using locuszoomr (v0.3.5) in R (v4.3.3). Forest plots of variant effects across *APOE* strata were generated using forestploter (v1.1.2) in R (v4.3.3). The independence of several signals within a locus was tested by conditional analysis in the five largest cohorts (EADB TOPMed, FINNGEN, UKB, GR@CE, ADSP) and meta-analyzed.

Stratified effect comparison tests

Two different tests of stratified effect comparisons between autosomal variants and the *APOE* strata were performed using summary statistics results from the different *APOE* strata. *P*-value threshold for significance was determined using a Bonferroni correction for 29 regions of interest (including the 9 loci in common in both strata, the 9 and 7 loci found in the ε44 + ε43 and ε33 strata, respectively, and the four additional signals found in 4 of the 25 loci; $P < 0.05/29$ regions of interest = 0.0017). The first test analyzed the effect difference between the ε44 + ε43 and ε33 *APOE* strata. The effect difference was calculated in each cohort separately ($\Delta\beta_i = \beta_{i,\varepsilon44+\varepsilon43} - \beta_{i,\varepsilon33}$, i is the cohort, β is the autosomal effect estimated in the stratified GWASs), with the s.e. of the effect difference calculated as the square root of sum of squares of s.e. for the effects $\text{s.e.}_{\Delta\beta_i} = \sqrt{\text{s.e.}^2_{i,\varepsilon44+\varepsilon43} + \text{s.e.}^2_{i,\varepsilon33}}$. The effect differences were combined across studies in a fixed-effect meta-analysis with an inverse-variance weighted approach (METAL (v2020-05-05) software). The test was referred to as the dominant test because it tests whether the presence of an ε4 allele changes the effect of the autosomal variant (independent of the number of ε4 alleles). Forest plots for the

calculated effect difference in each cohort were provided to assess the robustness of the stratified effect comparison test across the cohorts. The second test was a fixed-effect model estimating the effect from the number of ε4 alleles—$\beta_{ij} = \gamma_0 + \gamma_{\varepsilon4}x_{ij} + \gamma_{cohort}C_{ij} + \varepsilon_{ij}$, where i is the cohort, j is the strata (ε33, ε43, ε44), β_{ij} is the autosomal effect, x_{ij} is the number of ε4 alleles (0,1,2), C_{ij} is the cohort, γ_0 is the intercept, $\gamma_{\varepsilon4}$ is the effect of one ε4 allele, γ_{cohort} is the cohort effect and ε_{ij} is the error term. The second model was referred to as the additive model and was estimated using R (v4.3.3) and metafor package (v4.6.0).

We performed mixed-effect sensitivity interaction models to test whether the stratified effect comparison results were prone to between-strata relatedness bias, which could be a potential bias in the FinnGen cohort. The models were specified as follows: dominant mixed-effect model—$\beta_{ik} = \gamma_0 + \gamma_k x_{ik} + u_i + \varepsilon_{ik}$, where i is the cohort, k is the strata (ε33, ε44 + ε43), x_{ik} is the strata (ε33, ε44 + ε43, categorical), γ_k is the strata effect ($\gamma_{\varepsilon43+\varepsilon44}$ is the reference) and u_i is the random effect; additive mixed model—$\beta_{ij} = \gamma_0 + \gamma_4 x_{ij} + u_i + \varepsilon_{ij}$, with the same notation as above. For calculating the effect difference, both the ε33 and ε44 + ε43 effects should be available for a cohort to be included in the analysis. In the other models, we included all available data, for example, the ε44 GWAS in the Bonn cohort was not performed due to power, but the data from the Bonn ε33, ε43 and ε44 + ε43 GWASs were included if the SNPs passed QC.

Genome-wide interaction testing

Interaction testing between *APOE* ε4 carrier status and autosomal genetic variants for association with clinical AD was conducted separately in the five largest cohorts (EADB TOPMed, FinnGen, UKB, GR@CE and ADSP) using logistic regression or mixed models with an additive genetic model. We implemented a gene–environment interaction framework, treating *APOE* ε4 carrier status as the exposure modifier. The aim of the analysis was to closely mimic the main analysis that contrasts the ε33 and ε44 + ε43 strata. A full multi-allelic gene–gene interaction GWAS across all *APOE* genotypes was regarded as outside the scope of this project.

APOE ε4 carrier status was defined as 0 for individuals in the *APOE* ε33 strata and 1 for individuals in the *APOE* ε44 + ε43 stratum. All other strata were excluded from the analysis. The model used for analysis was AD ~ SNP + *APOE* ε4 carrier + SNP × *APOE* ε4 carrier + age + sex + cohort-specific covariates. The software and the specific adjustments for the different cohorts are detailed in Supplementary Table 2. Results from the individual cohorts were QCed as described in the stratified GWAS and the SNP and SNP × *APOE*_ε4_carrier estimates were meta-analyzed separately using an inverse-variance weighted fixed-effect meta-analysis as implemented in METAL (v2020-05-05). The same significance threshold ($P < 2.5 \times 10^{-8}$) was used in the interaction model as in the stratified GWAS meta-analysis, as SNP and interaction terms constitute independent tests. In this setup, the reference level in the interaction model corresponds to the reference level in the *APOE* ε33 strata GWAS and hence $\beta_{\text{SNP}}^{\text{interaction}} = \beta_{\text{SNP}}^{\varepsilon33\text{strata}}$. Likewise, the estimated effect for an SNP in the *APOE* ε44 + ε43 strata corresponds to $\beta_{\text{SNP}}^{\varepsilon44+\varepsilon43\text{strata}} = \beta_{\text{SNP}}^{\text{interaction}} + \beta_{\text{SNP x }APOE_\varepsilon4_\text{carrier}}^{\text{interaction}}$ but with the reference value shifted by the *APOE*_ε4_carrier estimate $\beta_{APOE_\varepsilon4_\text{carrier}}^{\text{interaction}}$, which is independent of the individual SNP.

Pathway analysis

Pathway analyses were performed on each meta-analysis stratum result separately using FUMA (v1.6.1)[43]. As requested by FUMA, all variants were annotated with an rsID using VEP release 112 and then lifted to the GRCh37 assembly using the Picard LiftOverVcf tool (v3.1.1)[44]. Variants having no rsID or failing the lift to the GRCh37 assembly were removed from the analysis. Remaining variants were then uploaded to FUMA and the pathway analysis was performed by MAGMA (v1.08)[45] using two different windows to assign a variant to a gene—0 kb (main analysis) and a window of 35 kb upstream and 10 kb downstream (second analysis). To account for multiple testing, we computed a false discovery rate (Benjamini–Hochberg) based on the number of genes included in the analysis. Pathways having a q value of <0.05 in either of the two windows were considered significant.

eQTL analysis

We performed an *APOE*-stratified *cis*-eQTL mapping analysis (*APOE* ε33; $n = 342$ and *APOE* ε44 + ε43; $n = 130$) in the ROSMAP dorsolateral prefrontal cortex ($n = 560$) cohort to investigate association of the lead variant in the *DDHD1* locus (rs10131116) with the RNA expression of nearby genes in a 1-Mb window around the variant, following the methodology described as before[6]. For the *APOE*-stratified *cis*-eQTL mapping, the genetic principal components and the gene expression Probabilistic Estimation of Expression Residuals factors were calculated within the respective strata separately, and sex, first three gPCs and the Probabilistic Estimation of Expression Residuals factors (first 45 for *APOE* ε33 and first 15 for *APOE* ε44 + ε43) were included as covariates.

SMR

SMR was performed using the SMR software developed and maintained by the Yang Lab, with default parameters[46,47] using summary data from the *APOE* ε33 and *APOE* ε44 + ε43 strata GWAS. We used *cis*-eQTL data from five of the seven regions in the MetaBrain Consortium dataset (cerebellum, cortex, basal ganglia, hippocampus and spinal cord)[48]. We applied a significance threshold of pSMR_multi $< 6.12 \times 10^{-6}$, which corresponds to the Bonferroni-corrected value at $\alpha = 0.05$ for 8,166 unique genes tested across all regions. In addition, we filtered at a HEIDI P-value threshold of pHEIDI > 0.01 to remove associations with inferred pleiotropy and only kept results where the number of SNPs included in the HEIDI tests was >3 (nsnp_HEIDI > 3).

Reporting summary

Further information on research design is available in the Nature Portfolio Reporting Summary linked to this article.

Data availability

Summary statistics have been made available through the European Bioinformatics Institute GWAS Catalog (https://ftp.ebi.ac.uk/pub/databases/gwas/summary_statistics/GCST90861001-GCST90862000)—GCST90861026 (*APOE* ε44 strata GWAS), GCST90861027 (*APOE* ε43 strata GWAS), GCST90861028 (*APOE* ε44 + ε43 strata GWAS), GCST90861029 (*APOE* ε33 strata GWAS), GCST90861030 (*APOE* ε22 + ε32 strata GWAS), GCST90861031 (*APOE* carrier interaction GWAS).

Code availability

The software used is referenced in the online methods and the applied codes have been made available at https://github.com/JesperQT/APOEstratGWAS and via Zenodo at https://doi.org/10.5281/zenodo.21358786.

References

37. Vitale, D. et al. GenoTools: an open-source Python package for efficient genotype data quality control and analysis. *G3 (Bethesda)* **15**, jkae268 (2025).
38. Marchini, J., Howie, B., Myers, S., McVean, G. & Donnelly, P. A new multipoint method for genome-wide association studies by imputation of genotypes. *Nat. Genet.* **39**, 906–913 (2007).
39. Chang, C. C. et al. Second-generation PLINK: rising to the challenge of larger and richer datasets. *GigaScience* **4**, 7 (2015).
40. Mbatchou, J. et al. Computationally efficient whole-genome regression for quantitative and binary traits. *Nat. Genet.* **53**, 1097–1103 (2021).

41. Juliusdottir, T. topr: an R package for viewing and annotating genetic association results. *BMC Bioinformatics* **24**, 268 (2023).
42. Li, J. & Ji, L. Adjusting multiple testing in multilocus analyses using the eigenvalues of a correlation matrix. *Heredity (Edinb)* **95**, 221–227 (2005).
43. Watanabe, K., Taskesen, E., van Bochoven, A. & Posthuma, D. Functional mapping and annotation of genetic associations with FUMA. *Nat. Commun.* **8**, 1826 (2017).
44. McLaren, W. et al. The Ensembl Variant Effect Predictor. *Genome Biol.* **17**, 122 (2016).
45. De Leeuw, C. A., Mooij, J. M., Heskes, T. & Posthuma, D. MAGMA: generalized gene-set analysis of GWAS data. *PLoS Comput. Biol.* **11**, e1004219 (2015).
46. Wu, Y. et al. Integrative analysis of omics summary data reveals putative mechanisms underlying complex traits. *Nat. Commun.* **9**, 918 (2018).
47. Zhu, Z. et al. Integration of summary data from GWAS and eQTL studies predicts complex trait gene targets. *Nat. Genet.* **48**, 481–487 (2016).
48. De Klein, N. et al. Brain expression quantitative trait locus and network analyses reveal downstream effects and putative drivers for brain-related diseases. *Nat. Genet.* **55**, 377–388 (2023).

Acknowledgements

The authors thank the many study participants, researchers and staff for collecting and contributing to the data, the high-performance computing service at the University of Lille and the staff at CEA-CNRGH for their help with sample preparation and genotyping and excellent technical assistance. This work used the computational resources of the National Institute of Health (NIH) STRIDES Initiative (https://cloud.nih.gov) through the Other Transaction agreement—Azure: OT2OD032100, Google Cloud Platform: OT2OD027060, Amazon Web Services: OT2OD027852. This work also used the computational resources of the NIH HPC Biowulf cluster (https://hpd.nih.gov). Part of this research has been conducted using the UKB Resource under application 33601, and this work uses data provided by patients and collected by the National Health Service as part of their care and support. H.L. is a collaborator on UKB application 33601 and had access to the data under this approved project. Information for the consortia—acknowledgments, funding and list of members—is provided in the Supplementary Note.

Author contributions

J.Q.T., H.L., B.U., B.G.-B., J.-C.L., C.v.D., M.N. and R.F.-S. conceptualized and designed the study. J.Q.T., H.L., B.U., B.G.-B., S.H., P.G.-G., A.C.-M., M.K., J.G., H.C., F.K., N.A. and D.Y. conducted the data analysis. J.Q.T., H.L., B.U., B.G.-B., S.H., P.G.-G., A.C.-M., M.K., J.G., H.C., F.K., N.A., D.Y., I.d.R., P.A.J., V.A., B.A., C. Bellenguez, S.B., K.B., C. Blauwendraat, M.B., B.B., P.B., M.J.B., A.D., Á.C., A.d.M., M.C., J.D., M.D., S. Djurovic, O.D.-I., C.D., E.D., V.E.-P., T.F., L.F., A.K.Y.F., D.G., J.M.G.-A., V.G., G.G.-R., C.G., T.G., E.G., O.H., L.H., S.H.-H., J.H., F.J., K.J., C.J., Y.K., N.K., V.L., A.L., J.L., M.M., H.M., C.M., P. Mecocci, S. Mehrabian, P. Mir, A.M., S. Moebus., K.Y.M., L.M.P., F.M., B.N., L.P., P.P., J.P.-T., O.P., Y.A.L.P., G.P.-R., J.P., I.R., L.M.R., S.R.-H., E.R.-R., A. Rongve, G.R., J.L.R., D.R., I.S., M.E.S., R.S.-V., F.S.-G., N. Sandau, N. Scarmeas, K. Scheffler, N. Scherbaum., A. Schneider, G.S., D.S., V.S., M.S., A. Squassina, E.S., N.T., L.T., K.P.T., W.M.v.d.F., J. Williams, J. Wiltfang, D.A., A.B.S., P.A., S. Debette, M.T., G.N., S.v.d.L., H.H., M.V.F., P.G.K., K. Sleegers, M.I., R.G., O.A.A., P.A.H., P.S.-J., R.S., N.Y.I., K.H.L., T.I., A. Ramirez, A. Ruiz, M.H., J.-C.L., C.v.D., M.N. and R.F.-S. were responsible for sample contribution. J.Q.T., H.L., B.U., B.G.-B., F.K., N.A., J.-C.L., C.v.D., M.N. and R.F.-S. conducted the interpretation of data. J.Q.T., H.L., B.G.-B., J.-C.L., C.v.D., M.N. and R.F.-S. were in core writing group.

Funding

This work was supported by a grant (EADB) from the EU Joint Programme—Neurodegenerative Disease Research. INSERM UMR1167 is also supported by the INSERM, Institut Pasteur de Lille, Lille Métropole Communauté Urbaine and the French government's LABEX DISTALZ program (development of innovative strategies for a transdisciplinary approach to AD). This work was further supported by grants from the Lundbeck Foundation (R278-2018-804 to R.F.-S.), the Danish Heart Foundation and the Research Fund at Sygeforsikringen Danmark (2021-0245 to R.F.-S.). N.A. is supported by the NIH and Oxford-GSK Institute of Molecular and Computational Medicine (IMCM). C.v.D. is supported by the US NIH, NovoNordisk, the Oxford-GSK IMCM, Centre of Artificial Intelligence for Precision Medicines of the University of Oxford and King Abdul Aziz University, Alzheimer Research UK, UK National Institute for Health and Care Research Oxford Research Center (BRC), ZonMW (Delta Dementie) and Alzheimer Nederland. This research was also supported in part by the Intramural Research Program of the NIH, National Institute of Aging, National Institutes of Health, Department of Health and Human Services (project ZO1 AG000534), as well as the National Institute of Neurological Disorders and Stroke.

Competing interests

C.v.D. is currently the Research Director of Brain Health at the Health Data Research UK and the UK Dementia Research Institute, working in partnership with Dementias Platform UK. Some authors' participation in this project was part of a competitive contract awarded to DataTecnica by the NIH to support open science research. M.N. also owns stock in Character Bio and Neuron23. The other authors declare no competing interests.

Additional information

Extended data is available for this paper at https://doi.org/10.1038/s41588-026-02713-9.

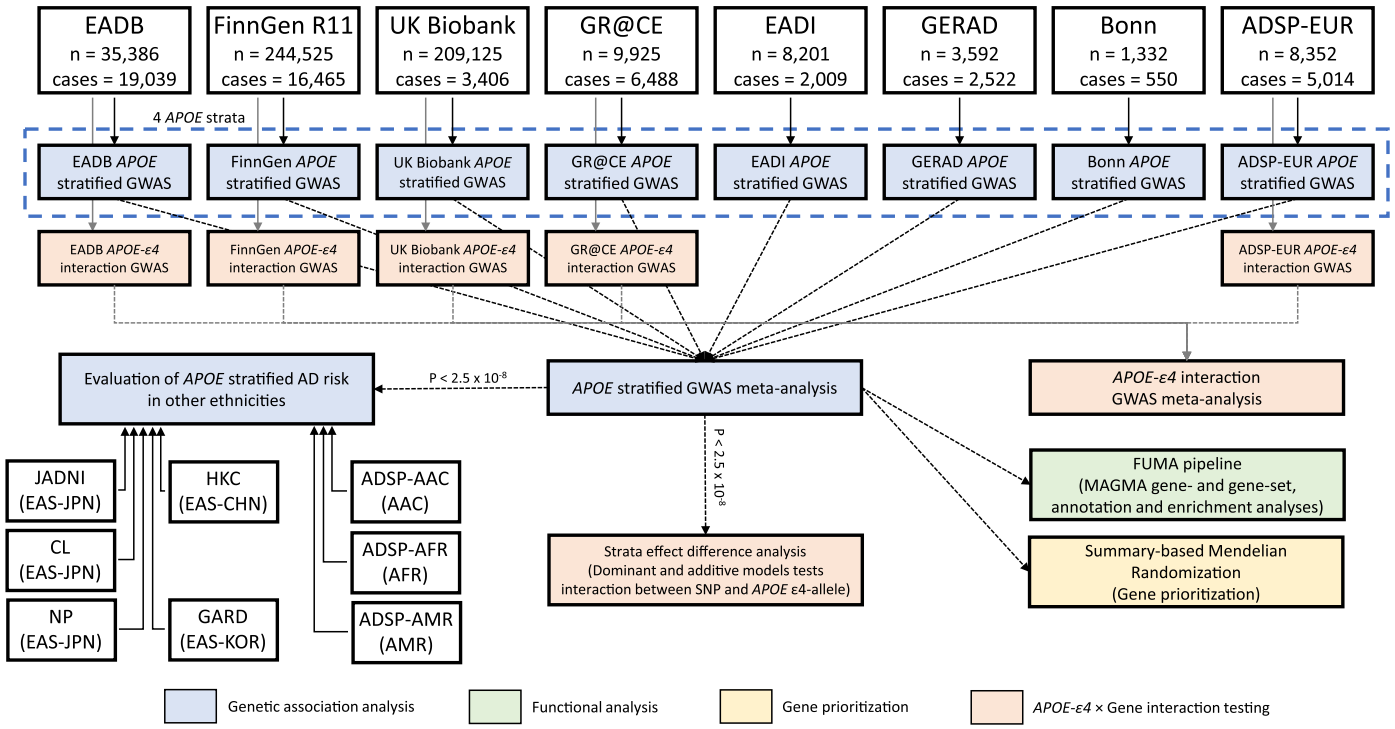
Supplementary information The online version contains supplementary material available at https://doi.org/10.1038/s41588-026-02713-9.

Correspondence and requests for materials should be addressed to Jesper Qvist Thomassen, Mike Nalls or Ruth Frikke-Schmidt.

Peer review information *Nature Genetics* thanks David Fardo, and Jin-Tai Yu for their contribution to the peer review of this work. Peer reviewer reports are available.

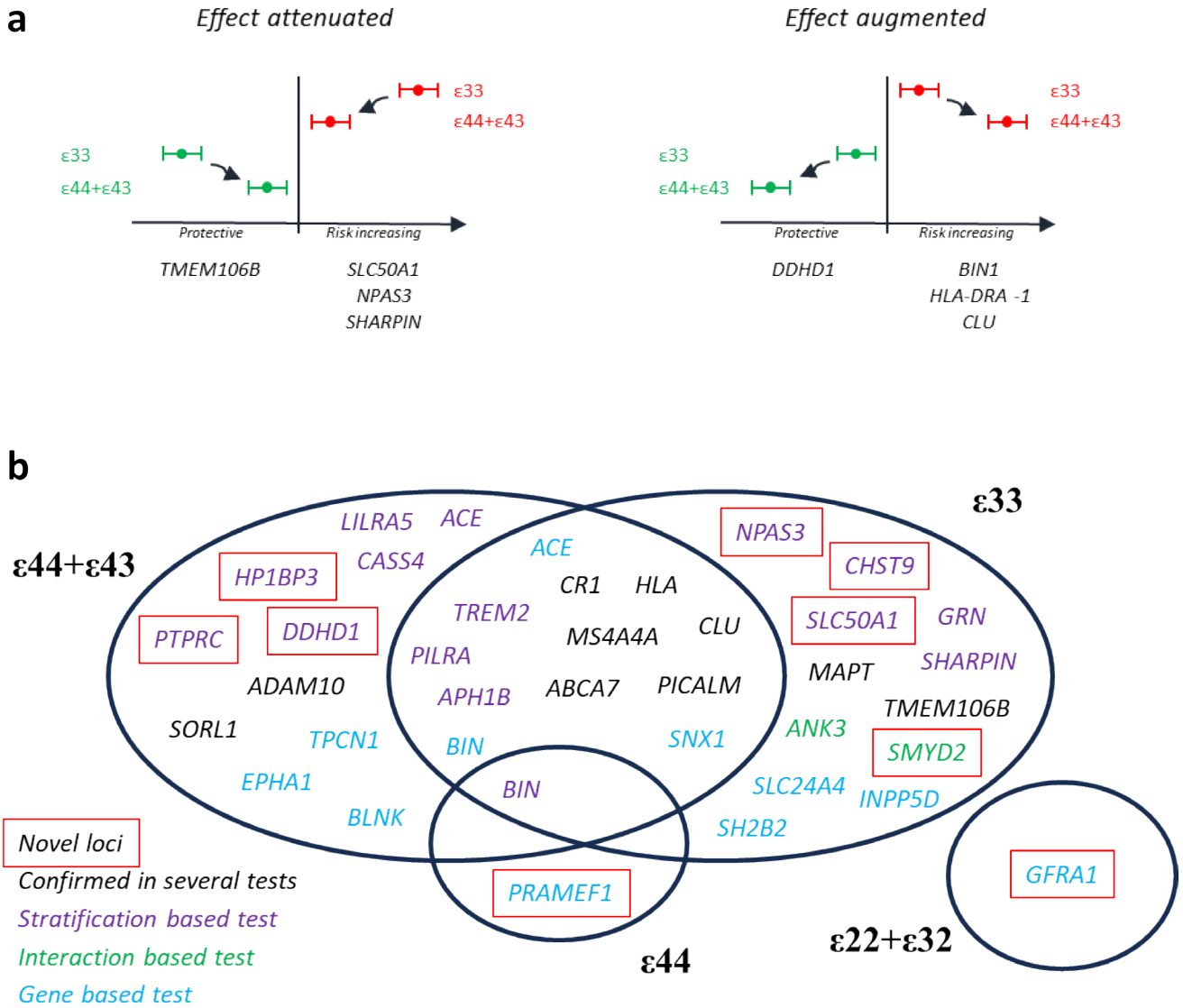
Reprints and permissions information is available at www.nature.com/reprints.

https://doi.org/10.1038/s41588-026-02713-9



Extended Data Fig. 1 | Flowchart of *APOE*-stratified GWAS analysis plan. Eight European, five East Asian and three American cohorts were included. Genetic association analysis (GWAS) was performed in four *APOE* strata (ε33, ε44, ε43 + ε44, ε22 + ε32). Genome-wide significant signals were tested with functional analysis, genetic characterization, and gene–gene interaction analysis.

https://doi.org/10.1038/s41588-026-02713-9



Extended Data Fig. 2 | Summary of findings. a, Summary of interaction findings. Left, illustrating attenuated protective and attenuated risk-increasing interaction effects for the *APOE*-ε4 allele. Right, illustrating the similar augmented protective and augmented risk-increasing interaction effects for the *APOE*-ε4 allele. Loci exhibiting the illustrated effect are noted below. The vertical line illustrates an odds ratio of 1 (no effect) and error bars illustrate confidence intervals. **b**, Venn diagram of the genome-wide significant loci associated with AD, showing the overlap between *APOE*-strata and between variant-based testing (stratified or interaction GWAS) and gene-based testing (MAGMA).

nature portfolio

Corresponding author(s): JQT, MN, RFS

Last updated by author(s): 29th June 2026

Reporting Summary

Nature Portfolio wishes to improve the reproducibility of the work that we publish. This form provides structure for consistency and transparency in reporting. For further information on Nature Portfolio policies, see our Editorial Policies and the Editorial Policy Checklist.

Statistics

For all statistical analyses, confirm that the following items are present in the figure legend, table legend, main text, or Methods section.

n/a	Confirmed	
☐	☒	The exact sample size (*n*) for each experimental group/condition, given as a discrete number and unit of measurement
☐	☒	A statement on whether measurements were taken from distinct samples or whether the same sample was measured repeatedly
☐	☒	The statistical test(s) used AND whether they are one- or two-sided *Only common tests should be described solely by name; describe more complex techniques in the Methods section.*
☐	☒	A description of all covariates tested
☐	☒	A description of any assumptions or corrections, such as tests of normality and adjustment for multiple comparisons
☐	☒	A full description of the statistical parameters including central tendency (e.g. means) or other basic estimates (e.g. regression coefficient) AND variation (e.g. standard deviation) or associated estimates of uncertainty (e.g. confidence intervals)
☐	☒	For null hypothesis testing, the test statistic (e.g. *F*, *t*, *r*) with confidence intervals, effect sizes, degrees of freedom and *P* value noted *Give P values as exact values whenever suitable.*
☒	☐	For Bayesian analysis, information on the choice of priors and Markov chain Monte Carlo settings
☒	☐	For hierarchical and complex designs, identification of the appropriate level for tests and full reporting of outcomes
☒	☐	Estimates of effect sizes (e.g. Cohen's *d*, Pearson's *r*), indicating how they were calculated

Our web collection on statistics for biologists contains articles on many of the points above.

Software and code

Policy information about availability of computer code

Data collection	Not relevant.
Data analysis	Custom code has been made available on https://github.com/JesperQT/APOEstratGWAS . Standard software has been used. SNPTEST v2.5.6 Regenie v2.-2.4.1 PLINK vv2.00a2-v.200a3.7 METAL v2020-05-05 R v4.3.3 topr (R package) v2.0.2 locuszoomr (R package) v0.3.5 forestplotter (R package) v1.1.2 Metafor (R package) v4.6.0 FUMA v.1.6.1 VEP 112 LiftoverVcf tool v3.1.1 MAGMA v1.08

For manuscripts utilizing custom algorithms or software that are central to the research but not yet described in published literature, software must be made available to editors and reviewers. We strongly encourage code deposition in a community repository (e.g. GitHub). See the Nature Portfolio guidelines for submitting code & software for further information.

Data

Policy information about availability of data

All manuscripts must include a data availability statement. This statement should provide the following information, where applicable:

- Accession codes, unique identifiers, or web links for publicly available datasets
- A description of any restrictions on data availability
- For clinical datasets or third party data, please ensure that the statement adheres to our policy

Summary statistics has been made available through the European Bioinformatics Institute GWAS Catalog: GCST90861026, GCST90861027, GCST90861028, GCST90861029, GCST90861030 and GCST90861031.

Research involving human participants, their data, or biological material

Policy information about studies with human participants or human data. See also policy information about sex, gender (identity/presentation), and sexual orientation and race, ethnicity and racism.

Reporting on sex and gender	Sex was adjusted for in the study. Sex was assigned based on genetic information.
Reporting on race, ethnicity, or other socially relevant groupings	The main study was made on individuals of European genetic ancestry. Main findings are further investigated in other genetic ancestry groups. This is due to the availability of data.
Population characteristics	Age, sex, genetic ancestry, APOE genotype, Alzheimer's diagnosis, genetic principal components.
Recruitment	Inclusion in the study was based on availability of data in already established cohorts.
Ethics oversight	Written informed consent was obtained from study participants or for those with substantial cognitive impairment, from a caregiver, legal guardian, or other proxy, and the study protocols for all the populations were reviewed and approved by the appropriate local institutional review boeard (see description of the samples in the supplementary information.)

Note that full information on the approval of the study protocol must also be provided in the manuscript.

Field-specific reporting

Please select the one below that is the best fit for your research. If you are not sure, read the appropriate sections before making your selection.

☒ Life sciences ☐ Behavioural & social sciences ☐ Ecological, evolutionary & environmental sciences

For a reference copy of the document with all sections, see nature.com/documents/nr-reporting-summary-flat.pdf

Life sciences study design

All studies must disclose on these points even when the disclosure is negative.

Sample size	The study included most of the largest Alzheimer's cohorts and biobanks available with participants of European ancestry and supplemented with cohorts of other ancestries.
Data exclusions	Samples and data were excluded based on standard quality control procedures as described in manuscript.
Replication	The meta-analysis strategy includes replication by default. Main findings were investigated in cohorts of other genetic ancestries.
Randomization	Samples were allocated into the experimental groups by Alzheimer's diagnosis and APOE genotype and the relevant covariates were adjusted for in the models applied..
Blinding	Blinding is not relevant in a GWAS study.

Reporting for specific materials, systems and methods

We require information from authors about some types of materials, experimental systems and methods used in many studies. Here, indicate whether each material, system or method listed is relevant to your study. If you are not sure if a list item applies to your research, read the appropriate section before selecting a response.

Materials & experimental systems

n/a	Involved in the study
☒	☐ Antibodies
☒	☐ Eukaryotic cell lines
☒	☐ Palaeontology and archaeology
☒	☐ Animals and other organisms
☒	☐ Clinical data
☒	☐ Dual use research of concern
☒	☐ Plants

Methods

n/a	Involved in the study
☒	☐ ChIP-seq
☒	☐ Flow cytometry
☒	☐ MRI-based neuroimaging

Plants

Seed stocks

Report on the source of all seed stocks or other plant material used. If applicable, state the seed stock centre and catalogue number. If plant specimens were collected from the field, describe the collection location, date and sampling procedures.

Novel plant genotypes

Describe the methods by which all novel plant genotypes were produced. This includes those generated by transgenic approaches, gene editing, chemical/radiation-based mutagenesis and hybridization. For transgenic lines, describe the transformation method, the number of independent lines analyzed and the generation upon which experiments were performed. For gene-edited lines, describe the editor used, the endogenous sequence targeted for editing, the targeting guide RNA sequence (if applicable) and how the editor was applied.

Authentication

Describe any authentication procedures for each seed stock used or novel genotype generated. Describe any experiments used to assess the effect of a mutation and, where applicable, how potential secondary effects (e.g. second site T-DNA insertions, mosiacism, off-target gene editing) were examined.